

The Pennsylvania State University

The Graduate School

**DYNAMIC INTERACTIONS BETWEEN THE CUTTING BLADE  
AND MISCANTHUS STEM**

A Thesis in

Agricultural and Biological Engineering

by

Zhankozy Toleu

© 2020 Zhankozy Toleu

Submitted in Partial Fulfillment

of the Requirements

for the Degree of

Master of Science

December 2020

The thesis of Zhankozy Toleu was reviewed and approved by the following:

Jude Liu

Associate Professor of Agricultural and Biological Engineering

Thesis Advisor

Charles David Ray

Associate Professor of Ecosystem Science and Management

Paul Heinemann

Professor of Agricultural and Biological Engineering

Head of the Department of Agricultural and Biological Engineering

## **Abstract**

The production of renewable energy has increased significantly in recent years due to global warming and national energy security needs. Among renewables, the biomass feedstock is a promising energy source. Dedicated energy crops, short-rotation woody crops, and agricultural crop residues are considered the primary biomass feedstocks, and existing harvesting, processing technologies and equipment for agricultural crops can be used. Miscanthus is a perennial energy crop, and research has indicated its high potential to become a primary feedstock for the bioenergy industry. However, since miscanthus is relatively new to the US renewable energy industries, the traditional harvesting and processing machines have not yet fully adapted to the production of this crop.

The feasibility of large-scale production of biomass crops for the bioenergy industry directly depends on the effectiveness of the harvesting and processing machines employed. High yield and stem rigidity of miscanthus complicate harvesting and processing and have caused high production costs. Thus, currently used traditional hay and forage machines may need to be modified to be suitable for this challenging crop. Improvement of harvesting, handling, and processing machinery efficiencies can be achieved by considering the mechanical and physical properties of this special crop during the machine design process. To understand miscanthus harvesting and size reduction processes, it is crucial to quantify the interactions between a cutting blade and the crop stem because cutting is a key process during harvesting, such as mowing, precutting when baling and grinding. Therefore, dynamic interactions between the cutting blade and miscanthus stem were studied in this research.

The effects of a blade type, sample supporting method, cutting speed, and stem location on cutting force and energy were studied. Serrated and flat blades, one side, and both sides

supporting method, upper and lower internode-node sections were tested during the experiment. The peak cutting force, the cutting energy and the cutting speed data were recorded.

Overall, for the flat blade, the average peak cutting force was 264 N, and the average cutting energy was 5.9 J. The average diameter of miscanthus samples used for the treatments with a flat blade was 9.5 mm. For the serrated blade, the average peak cutting force was 250 N, and the average cutting energy was 5.75 J. The average sample diameter was 9.33 mm with the serrated blade treatments. Blade cutting speeds for all treatments ranged from 8m/s to 11.3 m/s.

Statistical analysis showed that the blade type created significant differences in predicting specific cutting force ( $p=0.01$ ), while for the cutting energy ( $p=0.084$ ) blade type was not significant at a 95% confidence level. The stem location, whether lower or upper section of the whole plant stalk, was significant for specific cutting force, but specific cutting energy was not significant. Blade cutting speed was found to be not significant due to small cutting speed range. Finally, the stem section, whether it is node or internode, was significant in predicting the specific cutting force and the specific cutting energy.

# TABLE OF CONTENTS

List of Figures .....	viii
List of Tables .....	xi
Acknowledgments.....	xii
1. Introduction.....	1
2. Literature Review.....	4
2.1 Biofuels.....	4
2.2 Biomass.....	5
2.3 Energy Crops .....	6
2.3.1 Switchgrass .....	6
2.3.2 Willow.....	8
2.3.3 Miscanthus .....	10
2.4 Harvesting Methods and Equipment.....	11
2.5 Mechanical Properties and Mechanical Cutting of Crops .....	14
2.6 State of the Art .....	17
3 Goals. Objectives. Hypotheses .....	18
3.1 Goal.....	18
3.2 Objectives .....	18
3.3 Hypotheses.....	19
4. Methodology .....	21

4.1 Introduction.....	21
4.2 Miscanthus Sampling.....	22
4.3 High-Speed Impact Hammer .....	24
4.3.1 An overview of the device .....	25
4.3.2 Load cells and data logger .....	26
4.3.3 Speed sensor.....	27
4.3.4 Modification.....	28
4.4 Sample preparation .....	32
4.5 Laboratory Experiments and Data Collection.....	33
4.6 Data Analysis .....	36
5. Results and Discussion .....	38
5.1 Flat blade – one side supported.....	38
5.2 Flat blade – both sides supported.....	42
5.3 Serrated blade – one side supported.....	48
5.4 Serrated blade – both sides supported.....	54
5.5 Effect of Miscanthus Diameter on Cutting Force .....	58
5.6 Hypothesis testing.....	59
5.7 Statistical Analysis.....	62
5.8 Discussion.....	63
6 Conclusions and Recommendations .....	64

6.1 Conclusions.....	64
6.2 Recommendations.....	66
References.....	67

## List of Figures

Figure 2.1 - Switchgrass field .....	8
Figure 2.2 - Willow field .....	9
Figure 2.3 - Miscanthus field.....	10
Figure 2.4 - Reciprocating sickle bar mower (A), rotary disc mower (B).....	12
Figure 2.5 – Self-propelled (A) and pull-behind forage chopper .....	13
Figure 4.1 - Methodology overview flowchart.....	22
Figure 4.2 - Miscanthus research plots in Philipsburg, PA.....	23
Figure 4.3 - Collected miscanthus samples.....	24
Figure 4.4 - Front and side views of high-speed impact hammer.....	25
Figure 4.5 - Kistler 9712B load cell (A), Kistler data logger (B).....	26
Figure 4.6 - Speed sensor (A), GL-980 data logger (B) .....	28
Figure 4.7 - Load cells for reaction force measurements.....	29
Figure 4.8 – The hammer with two load cells (A), preliminary results (B) .....	30
Figure 4.9 – Fabricated flat blade used for the experiment .....	30
Figure 4.10 – Serrated blade used for the experiment .....	31
Figure 4.11 – Sample supporting methods (Johnson, 2012).....	31
Figure 4.12 – Unsupported cutting (A), one side supported cutting (B), two sides supported cutting (C).....	32

Figure 4.13 – Miscanthus samples prepared for the experiment .....	33
Figure 4.14 – Experiment treatment flowchart .....	34
Figure 4.15 – Peak cutting force illustration on the data points .....	35
Figure 5.1 – Illustration of cut sample using a flat blade with one side supported method .....	38
Figure 5.2 – Force-time curve of cutting in lower int. (A), lower no. (B), upper int. (C), upper no. (D) for the flat blade with one side supported method .....	39
Figure 5.3 – Effect of stem location on specific cutting force for the flat blade with one side supported method.....	41
Figure 5.4 – Effect of stem location on specific cutting energy for the flat blade with one side supported method.....	42
Figure 5.5 – Illustration of cut sample using a flat blade with both sides supported method.....	43
Figure 5.6 – Force-time curve of cutting in lower int. (A), lower no. (B), upper int. (C), upper no. (D) for the flat blade with both sides supported method .....	44
Figure 5.7 – Miscanthus internal structure along the stem. ....	46
Figure 5.8 – Effect of stem location on specific cutting force for the flat blade with both sides supported method.....	46
Figure 5.9 – Effect of stem location on specific cutting energy for the flat blade with both sides supported method.....	48
Figure 5.10 – Illustration of cut sample using a serrated blade with one side supported method	49
Figure 5.11 – Force-time curve of cutting in lower int. (A), lower no. (B), upper int. (C), upper no. (D) for the serrated blade with one side supported method .....	50

Figure 5.12 – Effect of stem location on specific cutting force for the serrated blade with one side supported method.....	52
Figure 5.13 – Effect of stem location on specific cutting energy for the serrated blade with one side supported method .....	53
Figure 5.14 – Illustration of cut sample using a serrated blade with both sides supported method. A- internode section, B – node section .....	54
Figure 5.15 – Force-time curve of cutting in lower int. (A), lower no. (B), upper int. (C), upper no. (D) for the serrated blade with both sides supported method. ....	55
Figure 5.16 – Effect of stem location on specific peak cutting force for the serrated blade with both sides supported method.....	56
Figure 5.17 – Effect of stem location on specific cutting energy for the serrated blade with both sides supported method.....	58
Figure 5.18 – Effects of miscanthus diameter on cutting force .....	59

## List of Tables

Table 5.1 – Peak cutting force summary for the flat blade with one side supported method.....	40
Table 5.2 – Cutting energy summary for the flat blade with one side supported method .....	41
Table 5.3 – Peak cutting force summary for the flat blade with both sides supported method....	45
Table 5.4 – Cutting energy summary for the flat blade with both sides supported method .....	47
Table 5.5 – Peak cutting force summary for the serrated blade with one side supported method	51
Table 5.6 – Cutting energy summary for the serrated blade with one side supported method.....	53
Table 5.7 – Peak cutting force summary for the serrated blade with both sides supported method .....	56
Table 5.8 – Cutting energy summary for serrated blade with both sides supported method.....	57
Table 5.9 – Statistical analysis results for flat and serrated blades.....	60
Table 5.10 – Statistical analysis results for one side and both sides sample supporting methods	61
Table 5.11 – Multiple linear regression analysis results.....	62

## **Acknowledgments**

I want to express my sincere gratitude for the following people who supported and helped during my M.S. study.

First of all, I would like to thank all Kazakhstan taxpayers for financially supporting my education through the “Bolashak” program under the Ministry of Education and Science. The knowledge, skills, and research experience I gained throughout my M.S. study will be beneficial for everyone.

I would like to thank Idaho National Laboratory for providing the high-speed impact hammer device which I used for my research.

I am sincerely grateful to my advisor Dr. Jude Liu for patiently supporting and guiding during my M.S. study. I appreciate his guidance, which led me to fulfill academic requirements and finish my thesis research. Moreover, I would like to thank Dr. Paul Heinemann and Dr. Charles David Ray for serving as committee members in my thesis research. I would also like to thank Dr. Roderick Thomas in the Department of Agricultural and Biological Engineering, and Penn State Learning Factory staff for helping me set up and modify the device I used for my experiments.

Most importantly, I would like to thank my family for their constant support and encouragement. Despite being thousands of miles away from them, I always felt their love and kindness during challenging times.

# 1. Introduction

Global warming, caused by greenhouse gas emissions that prevent the sun's heat from escaping the earth's surface, is one of the main concerns of humanity. According to US Environmental Protection Agency (2016), human activities that most contribute to greenhouse gas emissions in the USA are using conventional fuels for electricity (28.4%), heat (11%), and transportation (28.5%). As the data show, the primary source of greenhouse gases is human activities of burning fossil fuels. Moreover, it is expected that a crude oil shortage might lead to an energy crisis by 2060 (Technologies, 2013). One of the promising ways to reduce greenhouse gas emissions and dependence on conventional fuels is to substitute renewable energy sources for crude oil.

Biofuel is currently one of the environmental-friendly energy sources, which can replace conventional sources. It is predicted that in 45 years, biofuels will fulfill 30% of the world's energy needs (Guo et al., 2015). Ethanol is expected to have a brighter future among biofuels as a replacement for gasoline in the automobile industry. However, since the first-generation ethanol is made from food crops, the production of large quantities of ethanol is under question. Around 42% of harvested corn in 2012 in the US was used to produce ethanol, which covered only 10% of gasoline consumption (Guo et al., 2015). Such usage of crop grains for ethanol production is a potential risk for food security. Thus, second-generation biofuels where herbaceous (miscanthus and switchgrass) energy crops are being used to produce ethanol to reduce industry dependence on food crops. Herbaceous energy crops have advantages, such as converting sunlight energy into cellulose efficiently even when a low amount of fertilizers is

applied (Witzel and Finger, 2016), as well as the ability to grow with lower soil erosional losses and grow on marginal lands (Johnson, 2012).

Miscanthus has the potential to play a crucial role in the biofuel production industry because of its economic feasibility, high yields, and high fiber content. Miscanthus could produce three times more biomass and 2.5 times more gallons of ethanol per acre than other herbaceous energy crops (Heaton et al., 2008). Large-scale production of miscanthus would contribute boost to the agriculture and rural economy and promote using marginal lands common in the US (Fasick, 2013). However, high yield and stem rigidity make miscanthus challenging to harvest and process with existing machinery compared to other herbaceous crops (Johnson, 2012). According to Giampietro et al. (1997), the harvesting process dictates the feasibility of large-scale biofuel production from energy crops.

Interest in the massive production of energy crops for the biofuel industry has led researchers to review the energy efficiency of available traditional hay and forage machinery (Johnson, 2012). However, previous works have focused on existing harvesting machines by evaluating the energy required to harvest and to cut a single stem of conventional food and forage crops (Johnson, 2012). According to Shinnars et al. (2010), current harvesting machinery requires redesign to handle the high yields of energy crops. Thus, it is important to understand the harvesting process of energy crops, especially miscanthus, for large-scale production of energy crops and sustainable development of the bioenergy industry.

Mechanical and physical properties of biomass are significant features in developing and designing suitable harvesting and processing machines. Examining the mechanical and physical properties of energy crops will facilitate the design and development of efficient harvesting and processing machines.

These properties can be examined by applying various dynamic and static forces on a single crop stem. There are several studies on the mechanical properties of miscanthus measuring tensile and bending strength along a single stem. As only a few studies show, it is also important to evaluate interactions between a cutting blade and a single miscanthus stem by applying dynamic force to better understand harvesting and size reduction processes in a small scale. This thesis research is aimed to evaluate dynamic interactions between a cutting blade and miscanthus stem. Evaluating relationships between a cutting blade and miscanthus stem will facilitate understanding the engineering processes of biomass harvesting and size reduction. The goal of this research is to contribute to the development of efficient harvesting and grinding machines for the energy crops.

## 2. Literature Review

### 2.1 Biofuels

The enormous impact of fossil fuels on the environment and the expected shortage of petroleum-based fuel in 45, natural gas in 60 and coal in 120 years, much interest will be shifted in renewable energy (IEA, 2013). Thus, the US energy consumption picture is slowly changing back to the period before the 19th century when renewable energy was predominant. According to US Energy Information Administration (2018), fossil fuels generated four-fifth of the US energy demand in 2017, which is the lowest indication since 1902. Conversely, renewable energy consumption has been increasing since the 1910s, reaching its highest share 11.3% of total energy production in the US in 2017 (EIA, 2018). Undoubtedly, renewable energy will play a significant role in the US's energy security in the future.

Biofuels are accumulated energy sources derived from biomass feedstocks. Currently, solid, liquid, and gaseous-formed biofuels are commercially available. Firewood, wood chips, pellets, and charcoals are considered solid biofuels. Firewood used to be the primary energy source of humans for heating and cooking before discovering fossil fuel. However, firewood remains popular among some developing countries in Asia and Africa, where one-third of the population satisfies their energy demand by using firewood (Guo et al., 2015). A kilogram of well-dried firewood can generate energy equal to 15 MJ (ORNL, 2013). In the US 40 million m<sup>3</sup> of firewood was consumed in 2012 (FAO, 2013).

Another type of solid biofuels is wood chips. Unlike firewood, which is bulky, wood chips are small in size, which allows the use of smaller energy generation systems. Moreover, it is more convenient to transport and store chipped woods than bulky firewood. Wood chips have

been used as a biofuel since the beginning of the 21st century. Today, they are used to generate heat, hot water, and electricity. In 2012, the US generated 1.42% of its electricity from wood chips (EIA, 2013 Washington DC).

Wood chips can be further processed into pellets. The palletization process requires grinding dried wood crops or energy crops with a hammer mill to desired particle sizes, then compressing the mass into small cylindrical shapes. This process is not cost-effective, but it is efficient when importing abroad. The US exported 1.3 million tons of wood pellets to European countries in 2012 (IER, 2013).

Liquid biofuels are one of the few options to replace petroleum fossil fuels. Technological advancement facilitated the extraction of ethanol, biodiesel, and bio-oils from biomass feedstock. Thus, biomass and chemical composition of crops are the most important characteristics for sustainable biofuel production.

## **2.2 Biomass**

The Sun, wind, hydroelectric, and biomass are considered the main renewable energy sources. All of these primary renewable sources are being used to generate electricity, drive the transportation and industry. Among renewable sources, biomass accounts for the largest share of total energy consumption in the US. For example, biomass generated 45% of renewable energy, and it was 9% of the total energy use in the US in 2017 (EIA, 2018). Biomass can be converted into solid, gaseous, and liquid biofuels by using various technologies. In fact, biomass is the only renewable energy source from which liquid biofuel can be generated.

Today, agricultural crop residues, woody crops, dedicated energy crops, and animal waste are used as biomass feedstocks. It also includes some food crops such as corn, sugar cane,

wheat, soybean, and sugar beets. Growing attention on food crops as biomass feedstock stimulated farmers to increase acreages. It is estimated that biofuel industry used around 42% of corn grown in the US in 2012, and almost all corn is used to generate liquid biofuel (USDA, 2013). According to USDA, such interest in food crops for the renewable energy industry led to a price increase for some crops (USDA, 2015). Thus, there arises the question of whether food crops can fulfill the food security of human and animals, or can it be used as biomass feedstocks. In order to eliminate using food crops for biomass energy, researchers introduced second-generation biofuels where agricultural crop residues, short rotational woody crops, wood residue, organic waste, and dedicated energy crops are used as biomass feedstocks.

## **2.3 Energy Crops**

The primary purpose of the cultivation of dedicated energy crops is to fulfill a growing demand for biomass feedstock in renewable energy industries. Some examples of energy crops are switchgrass, miscanthus, willow, poplar, and reed canary grass. The following advantages make dedicated energy crops almost the perfect biomass feedstock to bioenergy industries. These crops are perennial, and only need to be planted once. Also, energy crops can grow with a low amount of fertilizers applied; they efficiently use water and nitrogen. Moreover, energy crops can be harvested several times a year, have high yields, and grow on marginal lands. Most importantly, energy crops do not compete with food production.

### **2.3.1 Switchgrass**

Switchgrass is one of the perennial energy crop types native to North America. US Department of Energy (DoE) selected switchgrass as a high potential model crop among 18

herbaceous crops, excluding miscanthus, for renewable energy production. The research conducted on searching potential bioenergy crops by seven institutions across the country from the 1980s to 1990s has concluded that switchgrass has a high potential to become the main biomass feedstock supply (Wright, 2007). According to Penn State Extension, establishing and harvesting processes of switchgrass accounted for the largest expenses of production cost.

Since switchgrass is a perennial crop, its establishment costs are high in the first year because of land preparation and planting processes. However, once planted switchgrass provides biomass up to 20 years long. Also, the necessity of fertilizer application boosts its establishment price. However, in consecutive years a low amount of fertilizer will be applied if there is no disease propagation.

Similarly, switchgrass is tolerant to extreme weather conditions, can grow in marginal lands and can provides high yield. The average yields of switchgrass are 10-15 tons per hectare and can reach 2 m tall each year. Moreover, it is established that switchgrass has a relatively similar chemical composition to corn and wheat crops, which is important for fermenting high-quality liquid and gaseous biofuels.

For bioenergy use, switchgrass harvesting is done in winter or early spring, although spring harvest can lead to dry matter losses. Harvesting can be accomplished with traditional harvesting equipment, and it is recommended to use self-propelled mowers with rotary cutting heads to mow to achieve high yields. After mowing, switchgrass is pressed to round or square bales to conveniently transport to biorefineries or storage facilities.



**Figure 2.1 - Switchgrass field**

<https://roundstoneseed.com/native-grasses/102-switchgrass.html>

### **2.3.2 Willow**

Historically, European immigrants started planting willow in New York and Pennsylvania states for basketry and furniture used in the 40s of the 19th century. Willow cultivation as biomass feedstock for bioenergy production in the US started from the mid of the 1980s (Keoleian and Volk, 2005). Today, willow is considered as a short-rotation woody energy crop. High yield, short growth cycle, disease resistance, and ability to grow after multiple harvests are characteristics that make willow ideal for bioenergy use. Also, willow grows in areas where soil moisture is high and prevents soil erosion. Besides energy generation, willow can be used as mulch, animal bedding, and fiberboard (Jacobson, 2013). There have been identified 107 willow species native to North America (Jacobson, 2013).

In the first year, willow grows up to 1.5 m and reaches 7.6 m consecutive years. Planted willow can be harvested once every three years up to 21 years, which is considered to be one of its main disadvantages. Willow can be harvested with traditional farm machinery, specialized with cutting head to a forage harvester (Jacobson, 2013). Generally, willow can be harvested using three different techniques (Kofman, 2012):

- whole-shoot harvesting
- chip harvesting (cut-and-chip)
- billet harvesting (cut-and-billet)

The purpose behind using the whole-shoot harvesting technique is to allow willow to dry naturally before it gets chipped. A disadvantage of this technique is dried willow's twigs becoming fragile, so during transportation and chipping processes, a lot of residues remain in the field.

In chip harvesting method, self-propelled machine or tractor-mounted equipment cuts and chops willow right away to the own trailer or to the trailer traveled alongside. Since willow is chopped without drying, in a few days, the high temperature might be developed in the biomass stack, which eventually might lead to the fire.

Billet harvesting is similar to the chip harvesting method. Although, chipped willow size in the billet method is 2-4 times larger than in the chip-harvested method. Its large sizes allow air to enter through biomass, so willow billets dry naturally.



**Figure 2.2 - Willow field**

[https://commons.wikimedia.org/wiki/File:Inside\\_a\\_field\\_of\\_willow\\_saplings\\_-\\_geograph.org.uk\\_-\\_1216382.jpg](https://commons.wikimedia.org/wiki/File:Inside_a_field_of_willow_saplings_-_geograph.org.uk_-_1216382.jpg)

### 2.3.3 Miscanthus

Miscanthus is another perennial crop, which showed promising potential to contribute sustainable development of renewable energy. Miscanthus is originated from Asia and considered as tropical and subtropical grass. In Europe and North America, miscanthus has been cultivating since the 1990s. Miscanthus is a bamboo-like crop with a stem diameter of 12-20 mm and a height of 3 m (Pyter et al., 2007). Illinois study plots demonstrated yields ranging from 6.2 to 14.8 Mg/ha, with the highest yield of 40 Mg/ha (Pyter et al., 2007).

Both methods, with traditional hay and forage harvesting equipment involved, field wilting, or direct-cut, are suitable to harvest miscanthus, with field wilting methods being the most popular. Harvesting and baling miscanthus is challenging compared to hay and forage crops because of the stiffness and rigidity of its stem. Miscanthus growing density - 5-10 plants per square foot complicates harvesting (Fasick and Liu, 2015). Thus, to increase harvesting and other production efficiencies, currently available equipment needs to be examined based on required properties. It will facilitate design and development of energy-efficient harvesting and size reduction machines for miscanthus.



**Figure 2.3 - Miscanthus field**

## **2.4 Harvesting Methods and Equipment**

The economic feasibility of large-scale production of biomass directly depends on harvesting methods and technology used during the process. Currently, dedicated energy crops are harvested with existing traditional forage and hay equipment. However, this equipment is not adapted to yield density, height, and stiffness of a particular energy crop, which results in a high cost of harvesting and size reduction processes. According to Lin et al. (2013), the harvesting process accounts for more than half of the total cost of biomass feedstock production. This section will focus on biomass harvesting methods, equipment, and some in-field studies on miscanthus harvesting.

Srivastava et al. (2006) divided harvesting into the following two methods: field wilting (mowing, conditioning, and baling) and direct-cut (chopping and transporting). These methods are most commonly used to harvest forage and hay crops. Both methods can be utilized on miscanthus and other energy crop harvesting. Since energy crops are dry enough, the in-field drying process can be eliminated.

The field wilting method is a sequence of mowing, conditioning, and baling processes. When a crop is grown to the desired maturity, mowers or mower-conditioners remove crops from the field. After harvesting with the mower, this method allows forage to dry in a field to the desired moisture content. Usually, ensilage and hay are baled and stored when a crop moisture content reduces to 50-65% and 15-23%, respectively (Johnson, 2012). When the field wilting method is used, effective harvesting of high-quality biomass depends on proper selection and installation of mower-conditioner. High-quality harvest accomplishes when yield mowing and collecting times are minimized. It is more critical to reduce the harvesting time of energy crops because they are usually harvested in winter times when weather conditions change hour-by-

hour. One of the ways to minimize harvesting time is to use advanced cutting mechanisms in mowers to improve the cutting process.

Based on cutting mechanisms, there are three types of mowers: reciprocating sickle bar mowers, vertical axis rotary mowers, and horizontal axis rotary mowers (Srivastava et al., 2006).

Figure 2.4 shows sickle bar mower and rotating disc mower.



**Figure 2.4 - Reciprocating sickle bar mower (A), rotary disc mower (B)**

<https://images.app.goo.gl/meMnHBGNDR2cMH3k9>. <http://sajware.com/equip/harvesting/discmower.html>

Sickle bar mowers have moving, and stationary blades lined up parallel to each other. The reciprocating mechanism allows to pinch a crop stem between moving and stationary blades and cut above the root. This type of mowers usually attached with the oblique angled serrated blades. The moving speed of a sickle bar mower depends on the growing density of a crop. In comparison with rotary disc type mowers, sickle bar mowers require less energy during the harvesting process.

Direct cutting is a combination of field wilting processes, which is done by forage chopper. However, field drying is not considered since forage is stored with existing moisture content. The chopping process includes mowing crops, gathering mowed mass to the chopper, and conveying mass to the track moving besides. Unlike the field wilting method, chopping

operations are done only with one equipment - forage harvesting machine. Two types of choppers are available: self-propelled (Figure 2.5 A) and pull-behind (Figure 2.5 B).

Generally, this method of harvesting is more time-efficient. However, some studies showed that its cost is higher than other available methods. Also, chopped biomass requires more storage space than baled biomass.

Unlike other crops, herbaceous crops are commonly harvested in late winter or early spring but could also be harvested in summer and fall. Thus, both methods can be used to harvest energy crops. According to the Ohio State University study, during the time between mowing and baling, miscanthus moisture increases while lying on the ground, which resulted in a baling process delay (Marrison, 2016). Thus, drying operation can be eliminated because of the adverse effect on subsequent operations. However, most forage and hay harvesting machines combine mowing and conditioning to reduce the drying time before baling.



**Figure 2.5 – Self-propelled (A) and pull-behind forage chopper**

<https://images.app.goo.gl/PSbKDhZSir8bEgzK7>

Field harvesting studies on miscanthus harvesting have been done. Gan et al. (2018) investigated the power consumption of miscanthus harvesting using a rotary mower-conditioner

with straight, angled, and serrated blade types. It was concluded that the blade type had a significant effect on the power consumption of harvesting equipment. Straight and angled blades required 24.7% and 18% more power than the serrated blade, respectively.

Another study investigated the effect of cutting speed, blade mounting method, and cutting blade type on energy consumption of miscanthus harvesting using a single disk cutter head platform (Maughan et al., 2014). Three different oblique angle blades ( $0^{\circ}$ ,  $30^{\circ}$ ,  $40^{\circ}$ ), and two mounting methods of blades, fixed and flexible were studied. The lowest average energy consumption of 9.1 MJ/ha was recorded using  $40^{\circ}$  oblique angle blade. Blades with oblique angle  $30^{\circ}$  and  $0^{\circ}$  resulted in average energy consumption of 16.9 MJ/ha and 23.1 MJ/ha. Overall, traditional hay and forage equipment have shown good results. However, the equipment still needs to be modified to high density and rigid structure of miscanthus crop, which resulted in slower operation of equipment (Anderson et al., 2011). According to previous studies, it is important to study static and dynamic cutting processes in order to evaluate traditional harvesting and size reduction equipment (Johnson et al., 2012).

## **2.5 Mechanical Properties and Mechanical Cutting of Crops**

Harvesting and processing energy crops, especially miscanthus and switchgrass, are complicated and costly because of low bulk density. Understanding the mechanical properties of these energy crops facilitates the design and development of suitable harvesting and processing machinery. One of the ways to measure mechanical properties is to apply static forces in longitudinal and transverse directions. Mechanical properties depend on moisture content, weather conditions, and harvest time. Relatively few studies were conducted on determining the mechanical properties of miscanthus.

For example, Liu et al. (2012) evaluated the mechanical properties of miscanthus. The experiment included shearing, tensile tests in cross-sectional and longitudinal directions, and bending tests. The shearing strength in cross-sectional and longitudinal directions were not significantly different. The mean shearing strength in the cross-sectional direction was 65 MPa, and the longitudinal direction was 7 MPa. The mean tensile strength in the cross-sectional direction was 1.1 MPa, and the longitudinal direction was 288.1 MPa. The results show that tensile failure requires more energy than shearing failure. After measuring the shearing and tensile forces of Switchgrass, Yu et al. (2006) concluded that grinding equipment with shearing failure force application is more energy efficient than tensile force.

Besides evaluating the mechanical properties of biomass, it is also important to evaluate static and dynamic cutting processes since plant materials act differently under tensile, compression, static, and dynamic loads (Persson, 1987). There have been a few dynamic and static cutting laboratory studies on a grass-like and cane-like biomass, including miscanthus, to investigate the effects of cutting blade types and cutting speed on cutting force and energy. Liu et al. (2012) have conducted a static cutting test on a single stem miscanthus to evaluate flat and serrated flat blades. During the experiment, cutting force and energy data were collected. The static force was applied to the lower internode section only. The cutting speed of the blades was 1.67 m/s. Liu et al. (2012) concluded that a flat blade required more force and energy to cut single stem miscanthus than a serrated flat blade. The average peak cutting force for the flat blade was 947 N, and the average cutting energy was 4.6 J. The average peak cutting force for the serrated flat blade was 615.3 N, and the average cutting energy was 3.6 J.

Johnson et al. (2012) conducted a study where they measured dynamic cutting energy on single stem miscanthus with three different blades ( $0^{\circ}$ ,  $30^{\circ}$ ,  $60^{\circ}$  oblique angles) at 10-20 m/s

range cutting speed. This was the only dynamic cutting study on miscanthus. The study showed that the energy required to cut miscanthus stem depends on blade type. The lowest average cutting energy of 7.62 J was acquired using a blade with a 60<sup>0</sup> oblique angle. The average cutting energy for straight and 30<sup>0</sup> blades were 8.73 J and 10.07 J, respectively. It was also found that cutting energy in node and internode sections was directly proportional to the cutting speed and the stem diameter.

Similar dynamic cutting studies were done on other grass-like and cane-like crops. For example, O'Dogherty and Gale (1991) evaluated dynamic cutting of ryegrass using cutting blade under the different oblique angles (0<sup>0</sup>, 15<sup>0</sup>, 30<sup>0</sup>, and 45<sup>0</sup>), and under the three different thickness of the blade (1 mm, 2 mm and 3mm). Cutting speed ranged between 15 to 35 m/s. The average diameter of ryegrass samples was 3.55 mm. It was concluded that the oblique angle of blades had no significant effect on cutting effectiveness above the critical cutting speed of 30m/s. The blade oblique angle had no significant effect on cutting force and energy, while the blade thickness had a small effect on cutting performance. However, a 3 mm thick blade required higher cutting specific energy below the critical speed. Also, a 1 mm thick blade took less time to cut a stem than 2 mm or 3 mm thick blades. Specific peak cutting force for all blades ranged between 6 N/mm to 14 N/mm. The average specific cutting energy above the critical cutting speed of 30 m/s was 87 mJ/mm<sup>2</sup>.

Moreover, Kroes and Harris (1996) measured peak cutting force and energy during the dynamic cutting of sugarcane stalk at 20 m/s blade speed. The diameter of the sugarcane samples ranged between 20 mm to 30 mm. Recorded peak cutting force ranged between 300 N to 700 N. While cutting energy ranged between 5 J to 25 J. The peak cutting force and energy were directly proportional to the sample diameter.

Another study was to evaluate the effect of blade type and cutting speed on cutting energy of maize stalk (Prasada and Gupta, 1975). The experiment was conducted using knives with 15<sup>0</sup>, 20<sup>0</sup>, 23<sup>0</sup>, 30<sup>0</sup>, and 35<sup>0</sup> bevel angles. The knife velocity ranged between 1.62 m/s to 3.95 m/s. The lowest cutting energy per unit area was acquired using a knife with 23<sup>0</sup> bevel angle at cutting speed between 2.5 m/s to 3 m/s.

## **2.6 State of the Art**

Miscanthus, as a dedicated energy crop, has emerged in the US market, and research attempts have started at the beginning of the 2000s. Currently, miscanthus productions are facing challenges with efficient harvesting, transportation, and processing operations, which resulted in high prices and low quality for biomass feedstock. High-efficiency harvesting and processing equipment will result in decreased costs of miscanthus production.

Traditional hay and forage harvesting equipment are not fully adapted for dedicated energy crops. Mechanical properties of energy crops, in this case miscanthus, need to be evaluated properly to modify traditional harvesting and size reduction equipment. A literature review indicates that there are a few studies conducted on the dynamic cutting test of miscanthus and other energy crops. By applying dynamic force on miscanthus, stem can be determined cutting force and energy requirements. Collected data will help to better understand harvesting and size reduction processes.

### **3 Goals. Objectives. Hypotheses**

Sustainable renewable energy production requires a low cost and high-quality supply of biomass feedstock all year long. Dedicated energy crops such as switchgrass and miscanthus have promising potential to supply low cost and high-quality biomass feedstock to biorefineries. However, drawbacks in harvesting, transportation, and processing operations of these crops do not fulfill requirements in renewable energy. Thus, technology and equipment used to process energy crops need to be examined. Furthermore, all processing equipment needs to be adapted under specific characteristics of dedicated energy crops such as miscanthus, willow, or switchgrass.

#### **3.1 Goal**

The goal of this research is to examine dynamic interactions between a cutting blade and miscanthus stem in transverse directions. Understanding dynamic relationships between a cutting blade and miscanthus stem will help to examine the efficiency of currently used equipment for miscanthus harvesting and size reduction.

#### **3.2 Objectives**

- To measure the cutting force and energy in node and internode for lower and upper sections of miscanthus.
- To examine the effects of cutting blades on force and energy.
- To compare stalk support methods for the cutting tests.

### **3.3 Hypotheses**

Ho: Means of specific cutting force among miscanthus stem are not significantly different.

Ha: Means of specific cutting force among miscanthus stem are significantly different.

Ho: Means of specific cutting energy among miscanthus stem are not significantly different.

Ha: Means of specific cutting energy among miscanthus stem are significantly different.

Ho: Means of specific cutting force using flat blade are not significantly different from serrated blade.

Ha: Means of specific cutting force using flat blade are significantly different from serrated blade.

Ho: Means of specific cutting energy using flat blade are not significantly different from serrated blade.

Ha: Means of specific cutting energy using flat blade are significantly different from serrated blade.

Ho: Means of specific cutting force using one side sample supporting method are not significantly different from both sides sample supporting method.

Ha: Means of specific cutting force using one side sample supporting method are significantly different from both sides sample supporting method.

Ho: Means of specific cutting energy using one side sample supporting method are not significantly different from both sides sample supporting method.

Ha: Means of specific cutting energy using one side sample supporting method are significantly different from both sides sample supporting method.

## **4. Methodology**

### **4.1 Introduction**

Laboratory experiments were conducted on cutting miscanthus stems with a high-speed impact hammer. In this section, a detailed description of the materials and methods used for the research is presented. The research was divided into six phases, and the overview flowchart is shown in Figure 4.1. The first phase is collecting miscanthus samples from the field during spring harvesting time. Previously, there has been no research conducted on high-speed impact hammer. Thus, the second phase consists of setting up and modifying the high-speed impact hammer. In the third phase, miscanthus stems are prepared for the experiment, and the diameter of samples are measured. Fourth, a laboratory experiment is conducted on cutting miscanthus stem, during which the peak cutting force and cutting speed data were collected and the integration method was used to calculate cutting energy based on force and displacement curve. In the fifth phase, collected data is analyzed and interpreted to test the stated hypotheses. Finally, in phase 6, the conclusion and recommendations are made based on the analyzed data for further research attempts.

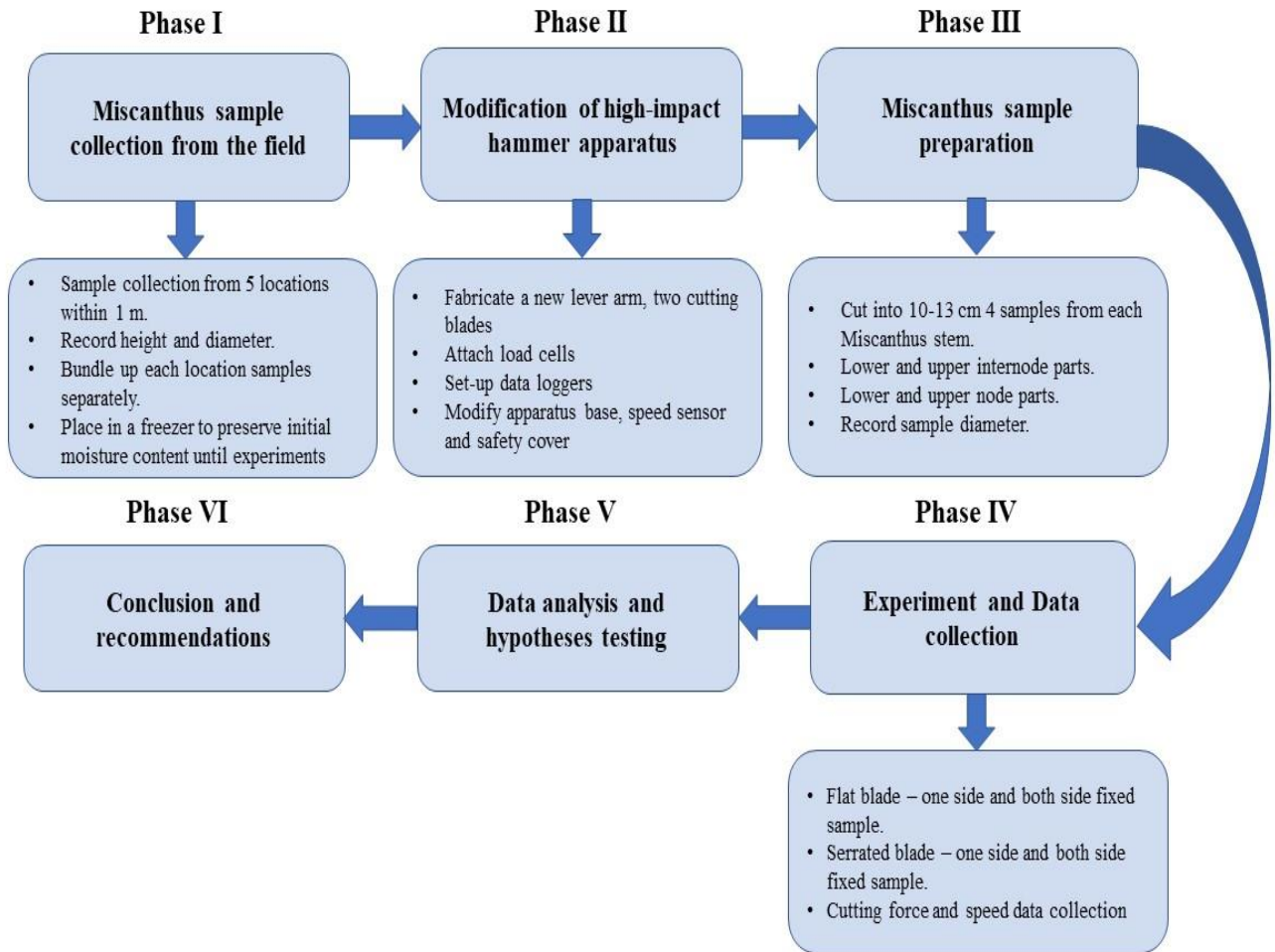


**Figure 4.1 - Methodology overview flowchart**

## 4.2 Miscanthus Sampling

The first phase of the research was collecting miscanthus samples from a field. Miscanthus samples used for the experiment were collected from experimental plots of The Pennsylvania State University located in Philipsburg, PA. There were two experimental plots of miscanthus in a total of 2 acres of land. Samples were collected in March 2019.



**Figure 4.2 - Miscanthus research plots in Philipsburg, PA**

The samples were collected from five random locations. At each location, plants were cut and collected from a one square meter area. It was collected 8.7 kg of 277 miscanthus plant samples from five locations. Based on collected samples, the average growing density of crops was 55 plants within one square meter area. Enough samples were collected in order to run a preliminary experiment to check if the load cells and data acquisition system work properly. The average height of the miscanthus samples was 2.4 m. Then, collected samples were separately bundled up by each collected area. In order to preserve the initial moisture content of the crop, all samples were stored in a freezer at  $-17^{\circ}\text{C}$  temperature until the experiment started.



**Figure 4.3 - Collected miscanthus samples**

### **4.3 High-Speed Impact Hammer**

A high-speed impact hammer located in the department of Agricultural and Biological Engineering at Penn State University, donated by the Idaho National Laboratory was used to measure dynamic shearing strength, power, and energy required to break a single stem biomass material. The purposes of developing this device was to better understand dynamic interactions between cutting tools and biomass feedstock materials such as corn stover, wheat straw, miscanthus, switchgrass, and willow. The front and side views of the high-speed impact hammer are shown in Figure 4.4.

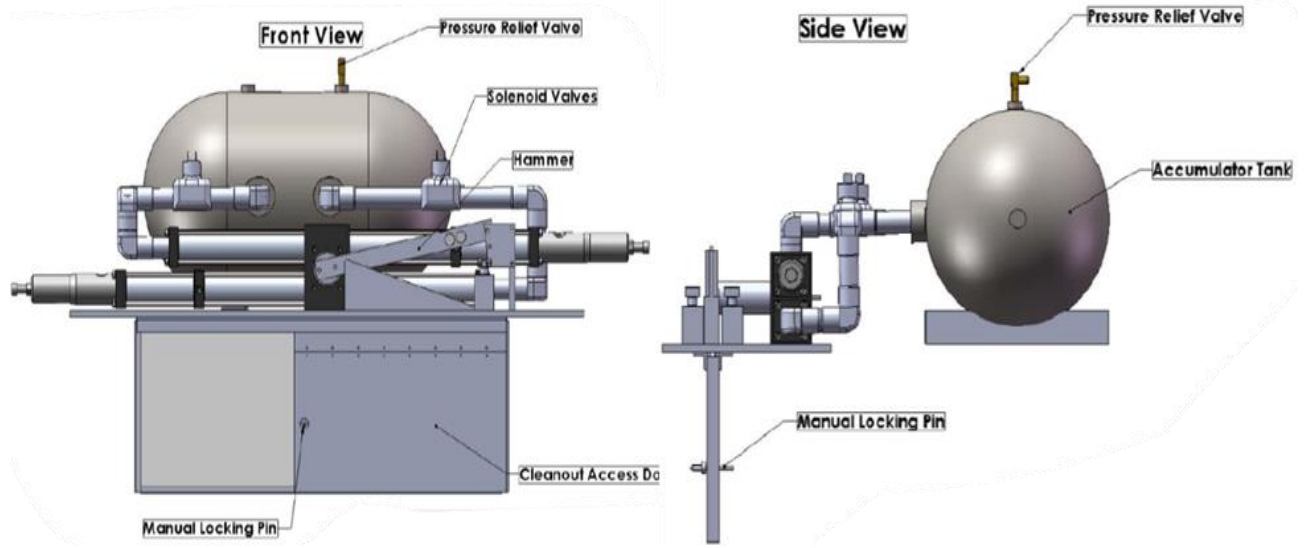


**Figure 4.4 - Front and side views of high-speed impact hammer**

### **4.3.1 An overview of the device**

The high-speed impact hammer has a pneumatically accelerated hammer using pressurized air supply. The hammer is propelled by a rotary actuator, which allows to spin a full 360°. The pressurized air is accumulated in an air tank with a capacity of 40 psi. The tank is continuously supplied with air from the building air pipeline system, during each cutting process, approximately 10 psi air pressure releases from the air tank. A control panel with supply and on/off buttons is used to accelerate the hammer.

The hammer can be attached with the different type of impacting and cutting tools. The starting point of the lever is vertically up. There are three magnets embedded in the arm which help to slow down after cutting a sample. The arm goes through the narrow aluminum and steel plates where slowing down process begins. In some cases, samples fall between the narrow pathway, so the front aluminum plate made as a door for cleaning purposes.

The rotary actuated hammer and pneumatic cylinders are firmly mounted on a thick steel plate. A slot cut on the plate parallel to the long axis allows the arm to rotate the full circle. The plate is attached to a large optical table and totally enclosed with polycarbonate for safety reasons. Polycarbonate allows to observe the cutting process. The apparatus is equipped with two anvils where test material places. Also, the apparatus is equipped with a time of flight sensors to measure cutting speed, which is mounted on the steel plate.

#### 4.3.2 Load cells and data logger

Kistler series 9712B piezoelectric low impedance load cells were used to measure cutting force (Figure 4.5). This type of sensors is developed to measure force where dynamic events are involved. The measuring range is from 5 lbf to 5000 lbf. Dynamic sensor calibration is an expensive process and needs special equipment. However, 9712B series sensors come with a calibration certificate. Thus, sensitivities provided from the manufacturer were used in the experiment.

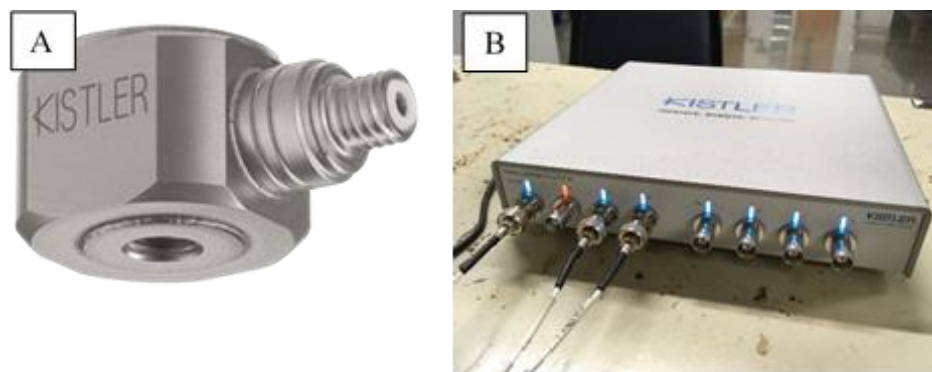


**Figure 4.5 - Kistler 9712B load cell (A), Kistler data logger (B)**

A sensor was placed between the hammer and cutting blade to measure the cutting force. The sensor was attached to Kistler data logger used to acquire data at a sampling rate of 200,000

samples per second. The load cell between the hammer and a cutting blade designated to measure the cutting force had a sensitivity of 0.248 mV/N.

The manufacturer also provides an online program to collect data directly to personal computer storage in EXCEL format. The online application allows automatically convert electrical shock signals from sensors to Newtons (N) or pounds per force (lbf) units.

### 4.3.3 Speed sensor

The time of the flight sensor is used to measure the speed of the cutting blade (Figure 4.6 A). The sensor has three pairs of emitter-receiver diodes that are lined up in a similar distance. The signal between emitter to receiver breaks when hammer travels through the emitter-receiver pathway. Thus, time passed from the first pair to the second, and the third pair was recorded at 100,000 samples per second. The cutting time data was collected using data logger GL-980 shown in Figure 4.6 B, which allows to collect data in EXCEL format. The cutting speed was calculated using a linear velocity formula.

$$v = \frac{S}{t}, m/s \quad (4.1)$$

where: S – distance between two emitting diodes, m

t – the hammer passing time from first diode to second, s

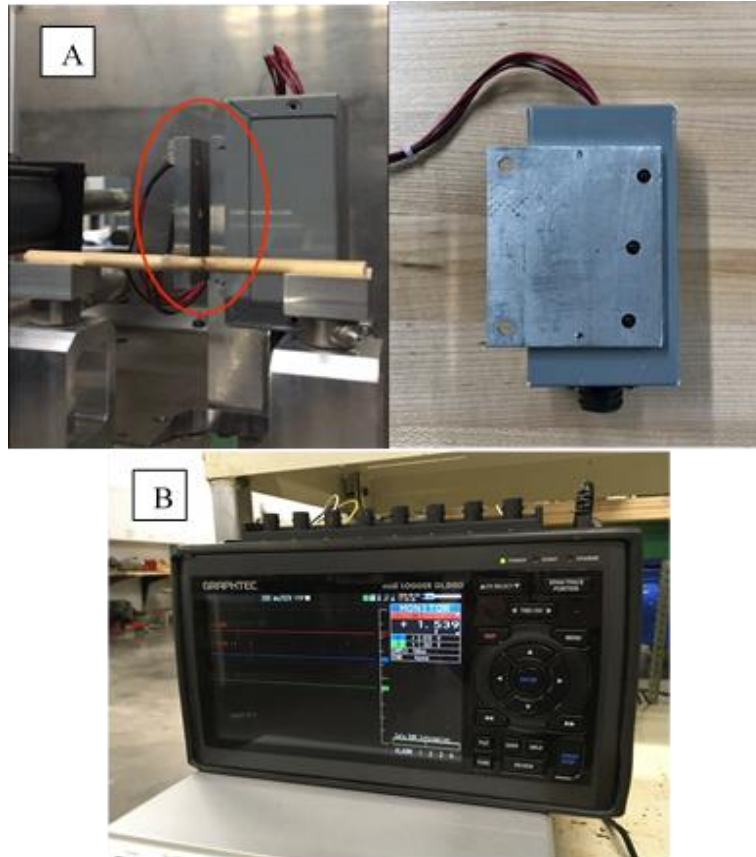


**Figure 4.6 - Speed sensor (A), GL-980 data logger (B)**

#### **4.3.4 Modification**

Some modifications were done on the high-speed impact hammer in order to measure cutting force. Originally, the device was developed to measure only cutting reaction force using two load cells under the v-shaped anvils where the sample is placed (Figure 4.7).

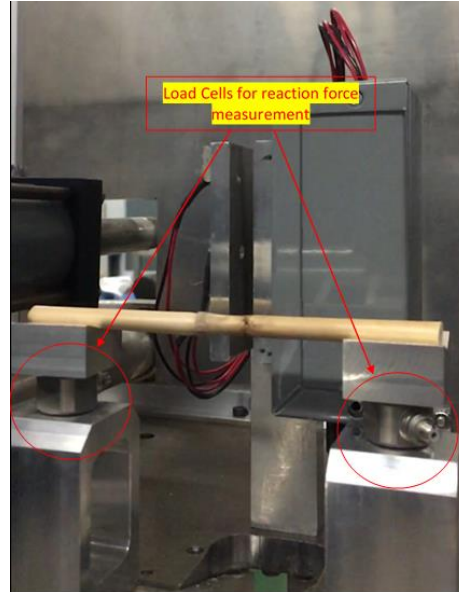


**Figure 4.7 - Load cells for reaction force measurements**

Additional two Kistler load cells series 9712B were purchased to attach between the hammer and cutting blade to measure the cutting force. The two sensors were attached to the newly fabricated hammer from a thicker aluminum bar since the old hammer could not fit 10-32 stud of sensors. It was expected that having two sensors will result in better results. However, preliminary cutting results showed that the sensor further from the cutting point does not receive any impact signals. The load cells used for the research only receive compression signals. Since momentum action comes to the one sensor, a second sensor subjects to tension force resulting in no signal. Thus, one sensor was removed, and the cutting blade was shortened. Figure 4.8 depicts attached two sensors on the hammer (A) and preliminary cutting test result (B). The orange curve represents data from the sensor attached further from the cutting point.

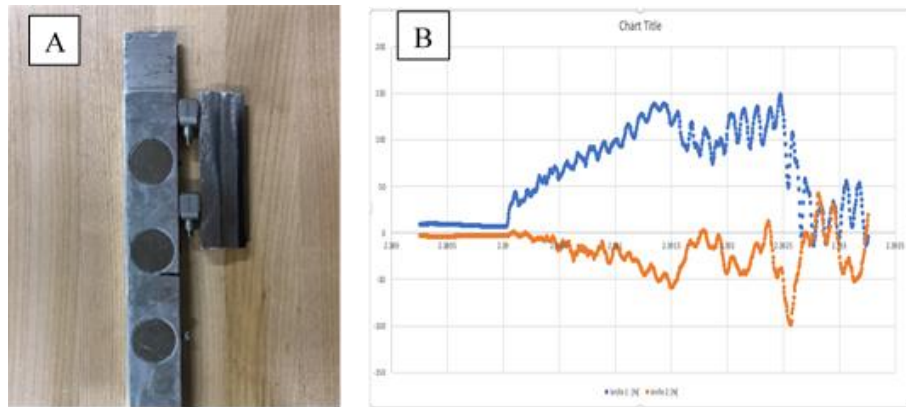


**Figure 4.8 – The hammer with two load cells (A), preliminary results (B)**

The apparatus has limited space to attach impacting and cutting tools. Original rotary disk mower and sickle bar mower blades do not fit available space in the device. Also, load sensors with 10-32 stud require at least a 0.625-inch flat surface, so this type of sensors cannot be attached to the thin blades. According to the original flat blade dimensions of a commercial rotary disk mower, a cutting blade was fabricated for this experiment so that the sensor can be attached. The dimension of the blade was minimized to reduce the effect of the blade momentum on the cutting force. The serrated blade was modified using a commercial blade to mount the sensor. Figure 4.9 shows a newly fabricated flat blade. The serrated blade used for the experiment also was modified to fit the space limitations of the device and sensor requirements. Figure 4.10 shows the modified version of the serrated blade.



**Figure 4.9 – Fabricated flat blade used for the experiment**

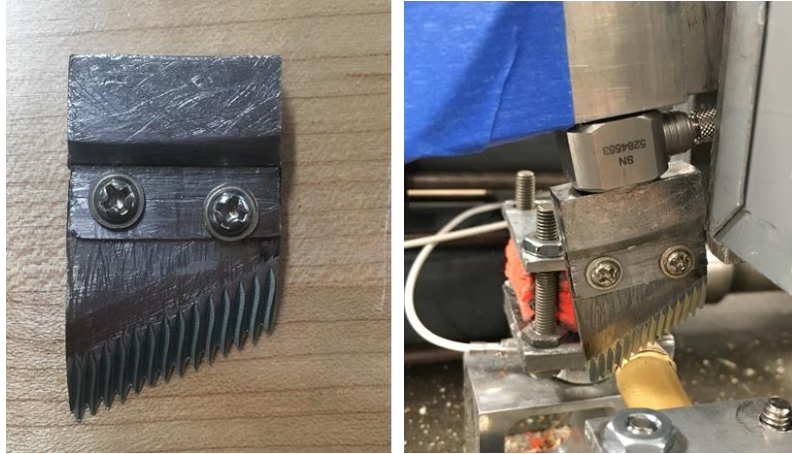


**Figure 4.10 – Serrated blade used for the experiment**

According to Johnson (2012), three cutting methods are currently used in harvesting machinery to cut hay and forage crops such as unsupported, one side supported, and both sides supported cutting (Figure 4.11). In the preliminary experiment, all three cutting methods were used.

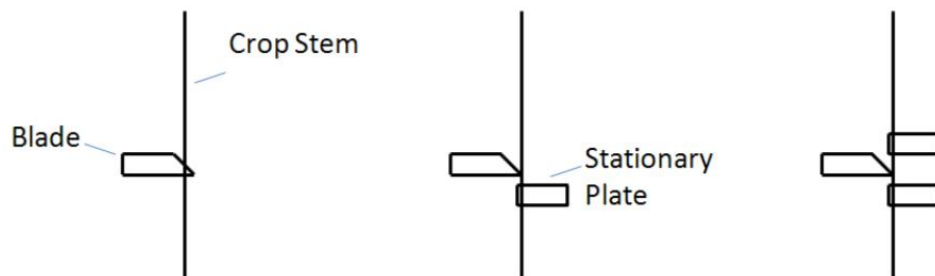


**Figure 4.11 – Sample supporting methods (Johnson, 2012)**

Srivastava et al. (2006) indicated that unsupported cutting requires 60-80 m/s cutting speed where cutting achieves by the inertia of the crop. The high-speed hammer used for the experiment has speed limitations because the braking system has a limited braking force to rapidly reduce the hammer swing speed after cutting. The maximum achieved cutting speed was

11 m/s. When the unsupported cutting method was used, the blades could not cut through the sample. Increasing the cutting speed could facilitated on better cutting when used unsupported method. However, the device does not have a proper braking system of the rotating hammer, as mentioned previously. Increasing the cutting speed will result in breaking down compression cylinders and the hammer. Thus, only two methods, one side, and two sides supported cutting were used in the experiment



**Figure 4.12 – Unsupported cutting (A), one side supported cutting (B), two sides supported cutting (C)**

#### **4.4 Sample preparation**

The third phase was the preparation of miscanthus samples for the experiment. The device was enclosed with acrylic glass for the purpose of safety. This limited room could not accommodate the whole miscanthus stem. Thus, each miscanthus sample was cut into four 13-15 cm long sections. It was cut into lower internode and node, upper internode and node, in order to test if cutting force and energy are significantly different in node and internode sections, as well in lower and upper sections. A total of 100 samples for 4 treatments was used in the experiment.

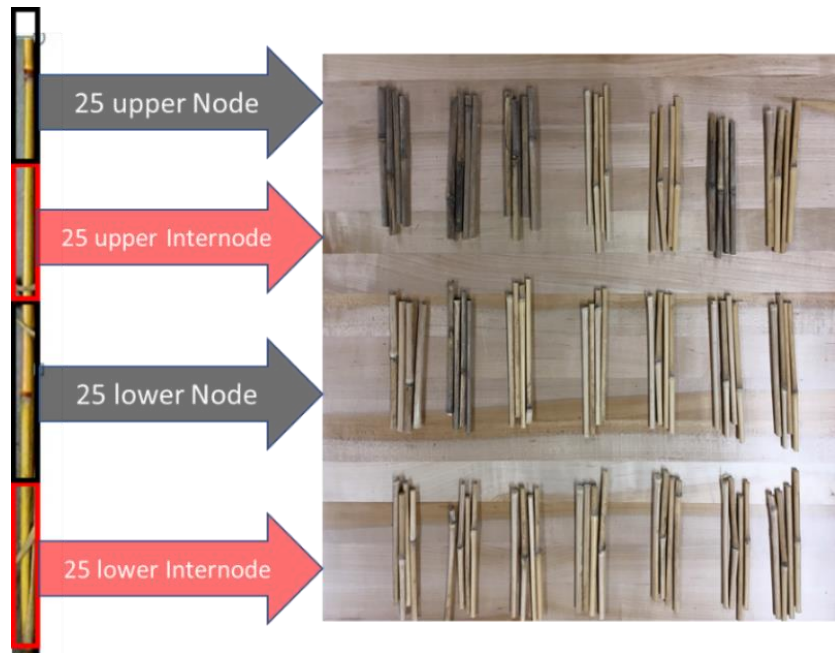


**Figure 4.13 – Miscanthus samples prepared for the experiment**

#### **4.5 Laboratory Experiments and Data Collection**

The fourth phase of the research was laboratory experiments to collect data using sensors and load cells and data acquisition system. The cutting force and cutting speed were measured using load cells and time of flight sensors, respectively.

The cutting force was collected using Kistler 9712B piezoelectric load cell attached between a cutting blade and the hammer. The data was collected at 200,000 samples per second rate using Kistler data logger and manufacturer online platform which automatically converts desired units to EXCELL format. Calibration of dynamic sensors is impossible without special devices. Thus, in this experiment the sensitivity of manufacturer 0.248 mV/N was used.

Each treatment had sub treatments such as lower internode, lower node, upper internode, and upper node. Each sub treatment had 25 replications. Thus, there were a total of 100 tests for each treatment. Figure 4.14 illustrates the detailed experiment treatments.

1. Flat blade with one side supported method.
2. Flat blade with both sides supported method.
3. Serrated blade with one side supported cutting method.
4. Serrated blade with both sides supported method.

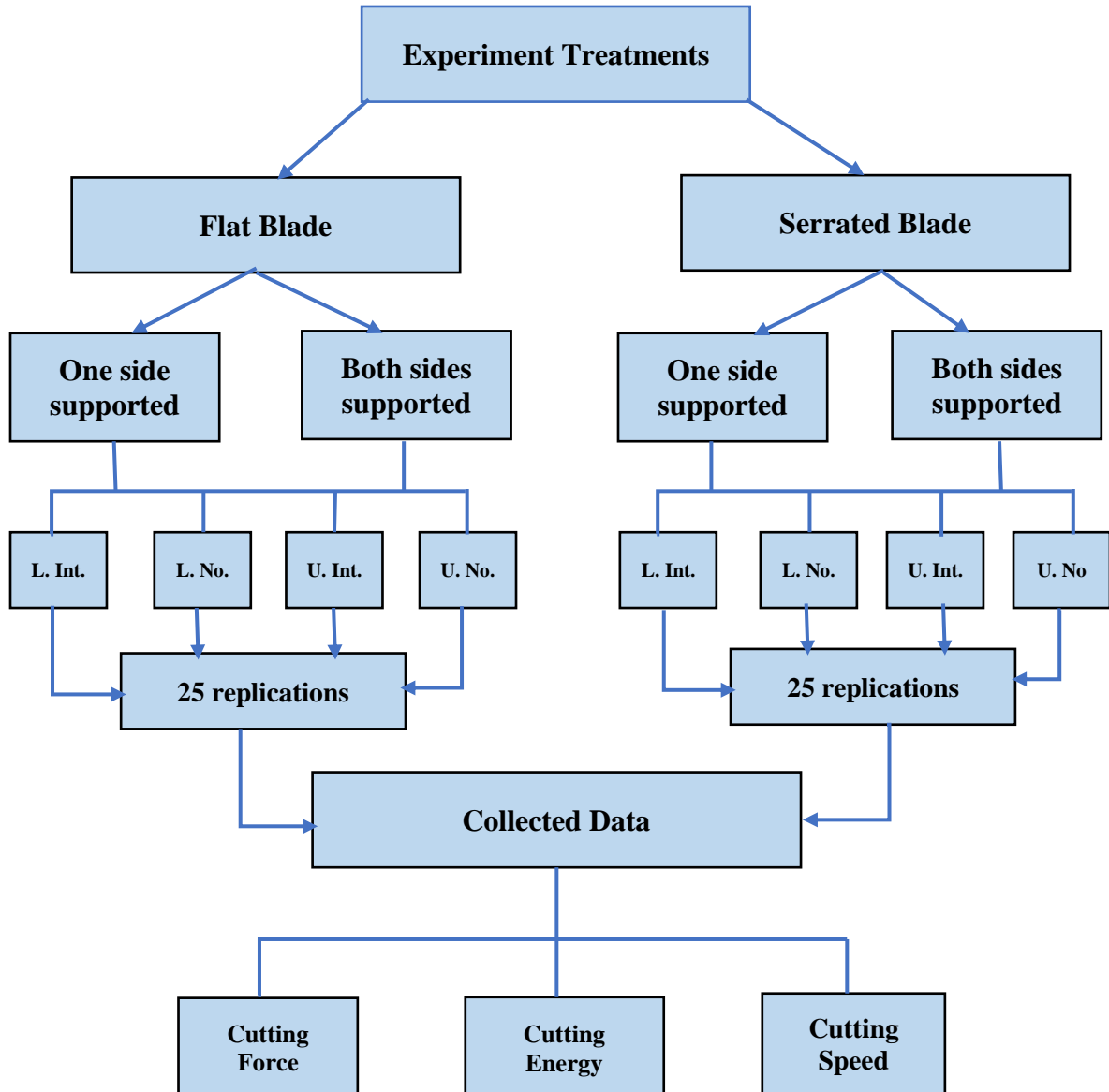


**Figure 4.14 – Experiment treatment flowchart**

The peak cutting force is represented as the maximum cutting force required to cut a single stem of miscanthus (Figure 4.15). The peak cutting force data were collected with a load cell attached between a hammer and a cutting blade. The load cell manufacturer Kistler provides an online program for the data acquisition system. The online program allows directly convert electrical signals from the load cells to the metric units. All data were collected in metric units and stored in EXCELL format.

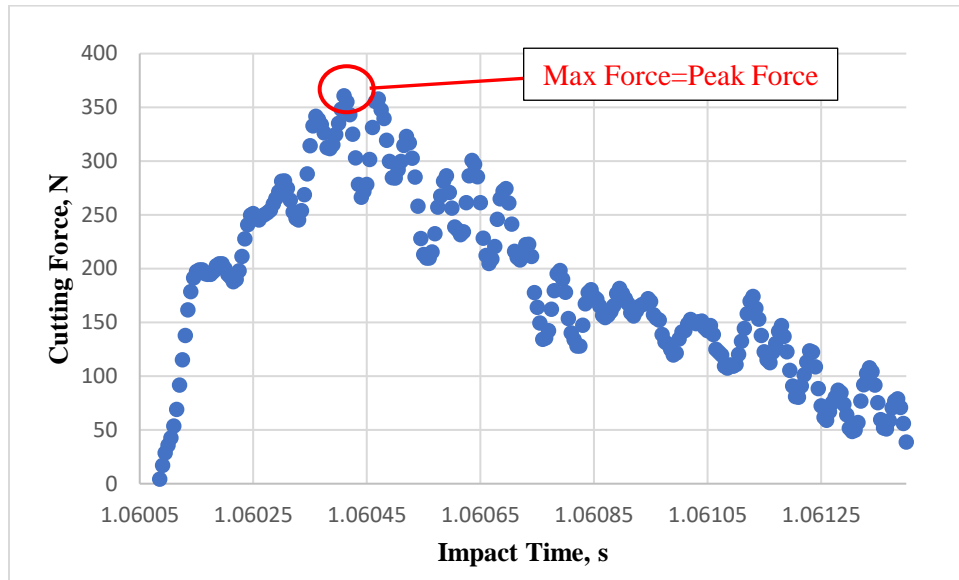


**Figure 4.15 – Peak cutting force illustration on the data points**

A stem cutting energy was calculated using the following formula (Vu et al., 2020):

$$E = P_c \times t, \quad (4.2)$$

where: E – the energy required to cut a single stem miscanthus, J

$P_c$  – power used during the cutting of single stem miscanthus, Watt

t – cutting duration of cutting pulse, s

The cutting power was calculated using peak cutting force and cutting speed, which were obtained from load cells and speed sensor. The following formula was used to calculate power (Vu et al., 2020):

$$P_c = F_{\text{peak}} \times V_c, W \quad (4.3)$$

where:  $P_c$  – cutting power, Watt

$F_{\text{peak}}$  – peak cutting force, N

$V_c$  – cutting velocity, m/c

Liu et al. (2012) represented the specific cutting force as the “force per unit diameter of the miscanthus stem”. Thus, the specific cutting force was found using the following formula:

$$F_{\text{sc}} = \frac{F_{\text{peak}}}{d}, N/m \quad (4.4)$$

where:  $F_{\text{peak}}$  – the peak cutting force, N

$d$  – diameter of the miscanthus stem, m

Researchers (Johnson et al., 2012) represented the specific cutting energy as the “energy per unit of stem diameter”. The specific cutting energy was found with the following formula:

$$E_{\text{sc}} = \frac{E}{d}, J/m \quad (4.5)$$

where:  $E$  – the cutting energy (Formula 4.2), J

$d$  – diameter of the miscanthus stem, m

## 4.6 Data Analysis

The cutting force, energy, and speed data were collected during the experiment. More specifically, the peak cutting force data, which was obtained using the Kistler load cells and data logger. The peak force represents the maximum force in the time-force curve, which shown in

the following sections. An online Kistler data logger program allows to convert electric shocks (volt unit) from load cells to the time-force curve in Newtons (N) or pounds per force (lbf) units in EXCEL format. The cutting energy was calculated with equations 4.2 and 4.3. The specific cutting force and energy data represent force and energy divided by the stem diameter in meters (m).

The fifth phase of this research is data analysis and hypothesis testing. Collected data were analyzed using one-way ANOVA and 2 sample t-tests using Minitab at a 95% confidence level. Also, linear regression analysis was conducted using STATA software. The purpose of this analysis is to examine whether the means of cutting force and energy among the stem are significantly different.

## 5. Results and Discussion

### 5.1 Flat blade – one side supported

The first experiment was carried out using a flat blade with one side supported cutting method. All samples for this treatment were randomly selected from the same bundle. The average moisture content of samples was 10.3% (w.b.), the average diameter of the used miscanthus specimens was 9.7 mm. The average cutting speed was 10.8 m/s. Despite a low cutting speed range 8.2 m/s – 11.3 m/s, the flat blade and one side supported method provided an effective and clear cutting as shown in Figure 5.1.



**Figure 5.1 – Illustration of cut sample using a flat blade with one side supported method**

The force-time characteristics of cutting the lower internode, lower node, upper internode, and upper node sections of a stem using the flat blade with one side supported method are illustrated in Figure 5.2. The majority of the acquired force-time characteristics had a similar pattern, but in some cases, the data was spread in an unusual pattern and produced some outliers. These outliers have affected a spread of peak cutting force means. This might be explained by high vibration from the pneumatic system of the device, which could adversely affect the sensor.

A similar problem occurred in the study where a high impact device was used, due to a high vibration of the impact cutting device, data acquired from the speed sensor could be inaccurate (Johnson, 2012).

The average cutting time of a stem cross-sectional area for this treatment was 0.0019 seconds. In most cases, the internodal cutting time was longer compared to the nodal cutting, where curves were sharp with shorter impact time. Despite the strong nodal section of miscanthus (Johnson, 2012), its impact time was less than for the internode section.

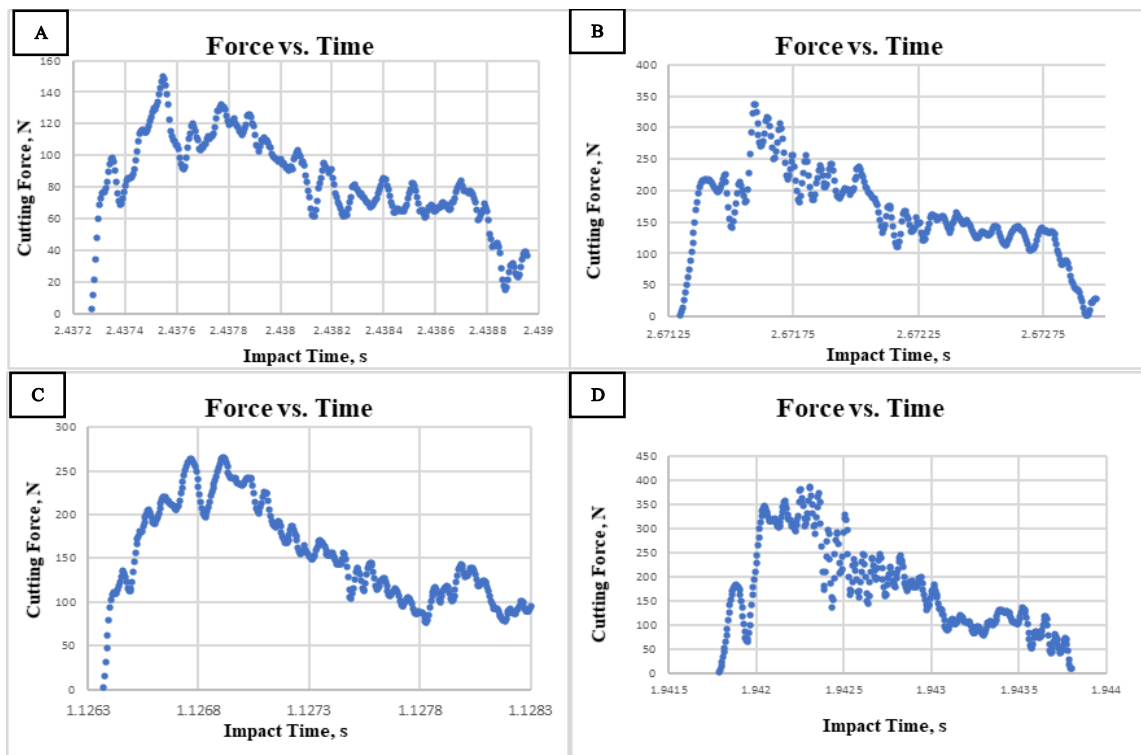


**Figure 5.2 – Force-time curve of cutting in lower int. (A), lower no. (B), upper int. (C), upper no. (D) for the flat blade with one side supported method**

Collected data, peak cutting force, cutting speed, and specimen diameter, using the flat blade with one side supported method is summarized in Table 5.1.

As shown in Table 5.1, the lowest specific cutting force of 21.6 kN/m is acquired at the lower internode section, while the highest 33.5 kN/m is acquired at the upper node section. These results agree with the statement that the nodal section of miscanthus tends to be harder than the internode section, so it requires more force and energy (Johnson, 2012).

**Table 5.1 – Peak cutting force summary for the flat blade with one side supported method**

Stem Location	Sample Size	Ave. Stem Diameter, mm	Ave. Cutting Speed, m/s	Peak Cutting Force, N		Specific Cutting Force, kN/m	
				Mean	SD	Mean	SD
Lower Int.	24	9.2	10.8	200	73	21.6	7.3
Lower No.	25	11.04	10.7	326	96	29.3	7
Upper Int.	24	8.5	10.9	211.7	57	25.1	6.4
Upper No.	24	9.8	10.9	330.4	85	33.5	7.4

One-way ANOVA test was used to test if specific force or specific energy means within stem location are significantly different ( $\alpha=0.05$ ). Tukey’s method in Minitab allowed comparing specific force or specific energy within 4 groups, in this case, lower internode and node, upper internode and node locations. This method was used to analyze each treatment individually. Upper case letters in Figure 5.3 illustrate the results of statistical analysis for specific cutting force within four stem sections. Based on statistical analysis, the specific cutting force in lower and upper internodes is not significantly different, as well as in node sections. Also, the means of the specific cutting force at the upper internode and lower node are not significantly different.

Thus, based on a one-way ANOVA analysis result, where the p-value was less than the significance level  $\alpha=0.05$ , the statement of the null hypothesis is rejected. The null hypothesis states that means of a specific cutting force at least in one location among miscanthus stem is significantly different from others when the flat blade with one side supported method was utilized.

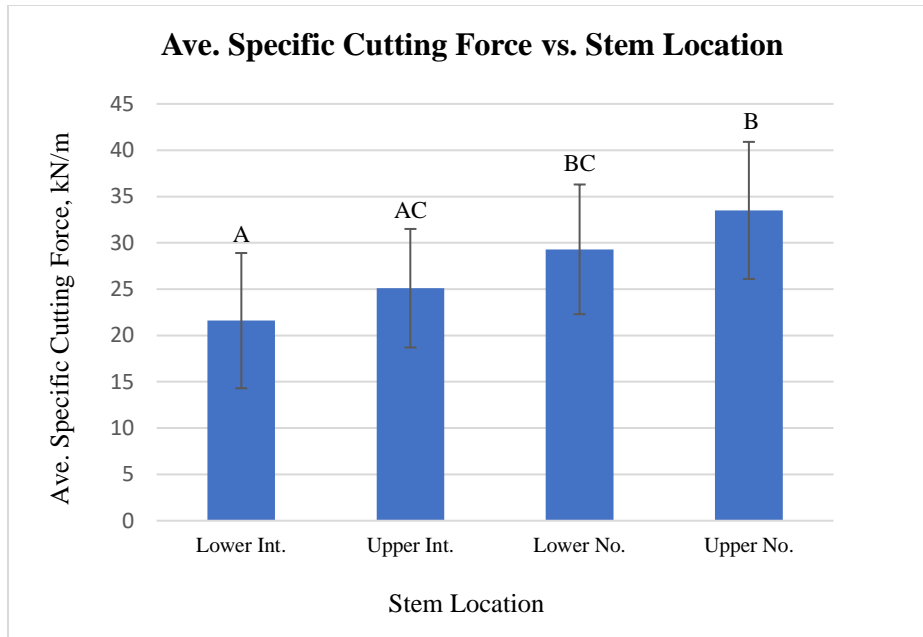


**Figure 5.3 – Effect of stem location on specific cutting force for the flat blade with one side supported method**

The cutting energy, which was calculated using formulas 4.2 and 4.3, as well as specific energy results are summarized in Table 5.2. The average cutting energy required to cut a single stem was 5.43 J. The lowest specific cutting energy acquired at the lower internode is 465.3 J/m, and the highest of 634.4 J/m is at the upper node.

**Table 5.2 – Cutting energy summary for the flat blade with one side supported method**

Stem Location	Sample Size	Ave. Stem Diameter, mm	Ave. Cutting Speed, m/s	Cutting Energy, J		Specific Cutting Energy, J/m	
				Mean	SD	Mean	SD
Lower Int.	24	9.2	10.8	4.3	1.8	465.3	167.6
Lower No.	25	11.04	10.7	6.6	2.3	588.0	162.2
Upper Int.	24	8.5	10.9	4.5	1.3	533.0	133.7
Upper No.	24	9.8	10.9	6.3	1.9	634.4	147.3

One-way ANOVA test results for specific energy within 4 stem locations are shown in Figure 5.4. The null hypothesis is rejected in all cases. The mean of the specific cutting energy is significantly different at least at one location ( $p=0.000$ ).

The average specific cutting energy at the lower and upper internodes is not significantly different. Moreover, average specific cutting energy at the lower and upper nodes, and at the upper internode is not significantly different.

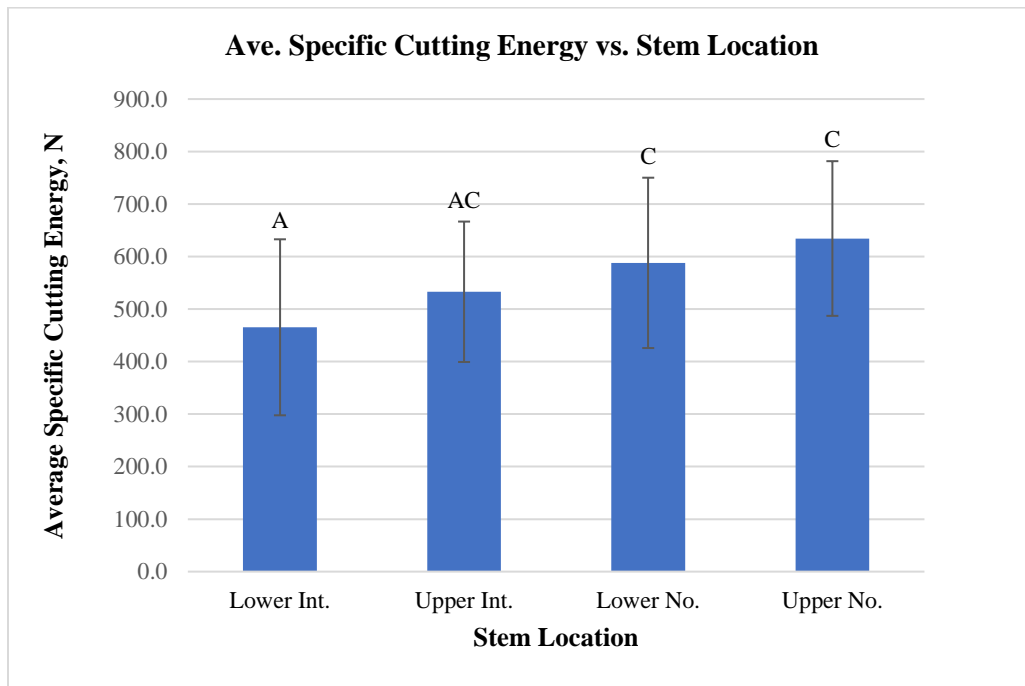


**Figure 5.4 – Effect of stem location on specific cutting energy for the flat blade with one side supported method**

## 5.2 Flat blade – both sides supported

The second experiment was conducted using a flat blade with both sides supported cutting method. All samples were randomly selected from one of the five collected bundles. The average moisture content of samples was 9.6% (w.b.). Miscanthus samples used for this treatment had the average diameter of 8.57 mm, and the average cutting speed of 10.8 m/s. This

cutting treatment provided a clear cut (Figure 5.5 A), but in some cases, samples were fractured and crushed (Figure 5.5 B), which was not observed in the flat blade with one side supported treatment.

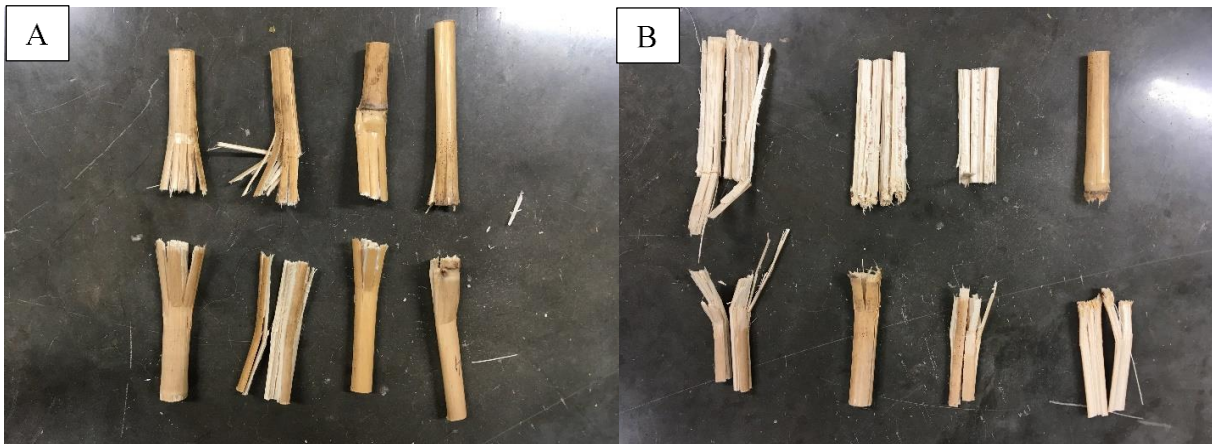


**Figure 5.5 – Illustration of cut sample using a flat blade with both sides supported method**

The force-time characteristics of impact cutting in 4 stem locations using the flat blade with both sides supported method are illustrated in Figure 5.6.

The average cutting time of a stem cross-sectional area for the particular treatment was 0.0024 seconds. Similarly, to the flat blade with one side supported treatment, internodal cutting had a wider force-time curve compared to nodal cutting, where curves were sharp with shorter impact time. However, the impact time was 20% longer compare to the flat blade with one side supported treatment. Therefore, fixing both sides of a sample had an impact on the length of cutting time.

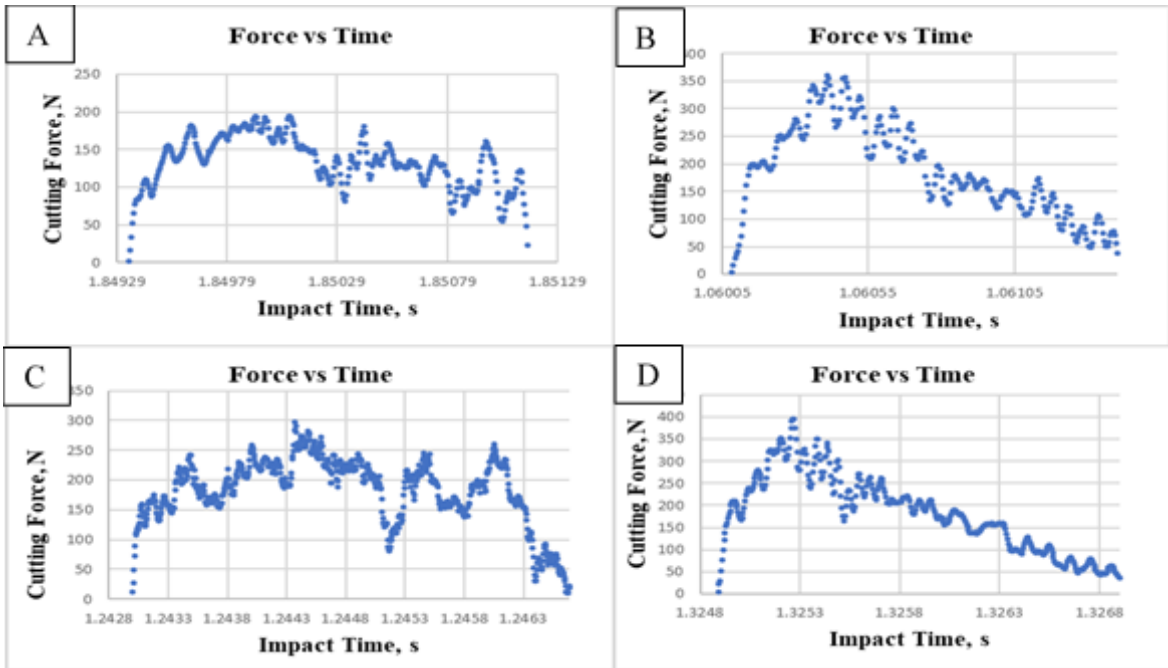


**Figure 5.6 – Force-time curve of cutting in lower int. (A), lower no. (B), upper int. (C), upper no. (D) for the flat blade with both sides supported method**

Collected data of peak cutting force, cutting speed, and sample diameter using a flat blade with both sides supported method is summarized in Table 5.3.

For both sides supported method, the specific cutting force was slightly increased by 8% compared to one side supported method. The lowest specific cutting force of 25.1 kN/m was observed at the lower internode section, while the highest 35.5 kN/m at the upper node section.

**Table 5.3 – Peak cutting force summary for the flat blade with both sides supported method**

Stem Location	Sample Size	Ave. Stem Diameter, mm	Ave. Cutting Speed, m/s	Peak Cutting Force, N		Specific Cutting Force, kN/m	
				Mean	SD	Mean	SD
Lower Int.	25	8.4	10.7	211	55.8	25.1	5.6
Lower No.	25	9.66	10.9	307.1	83.5	31.6	7.1
Upper Int.	25	7.5	10.8	210.3	60.6	27.7	5.7
Upper No.	25	8.7	10.8	310.8	80.9	35.5	6.7

Statistical analysis showed that means of specific cutting forces at least in one location is significantly different from others. Means of specific cutting forces at the lower and upper internodes are not significantly different, as well as at the lower and upper nodes. Mean specific cutting forces at the upper internode and lower node are not significantly different. However, it was expected that cutting the nodal section will have a significant effect on the specific cutting force than the internode section. Statistical analysis resulted to reject the null hypothesis. Thus, means of specific cutting force among miscanthus stem are significantly different when the flat blade with two sides supported treatment was used.

The internal structure of miscanthus along the stem might be an explanation for this phenomenon. It was observed that miscanthus samples used for the experiment came solid in the upper section while having a bamboo-like internal structure in the lower section. As shown in Figure 5.7, upper internode samples were solid from inside.



**Figure 5.7 – Miscanthus internal structure along the stem.**

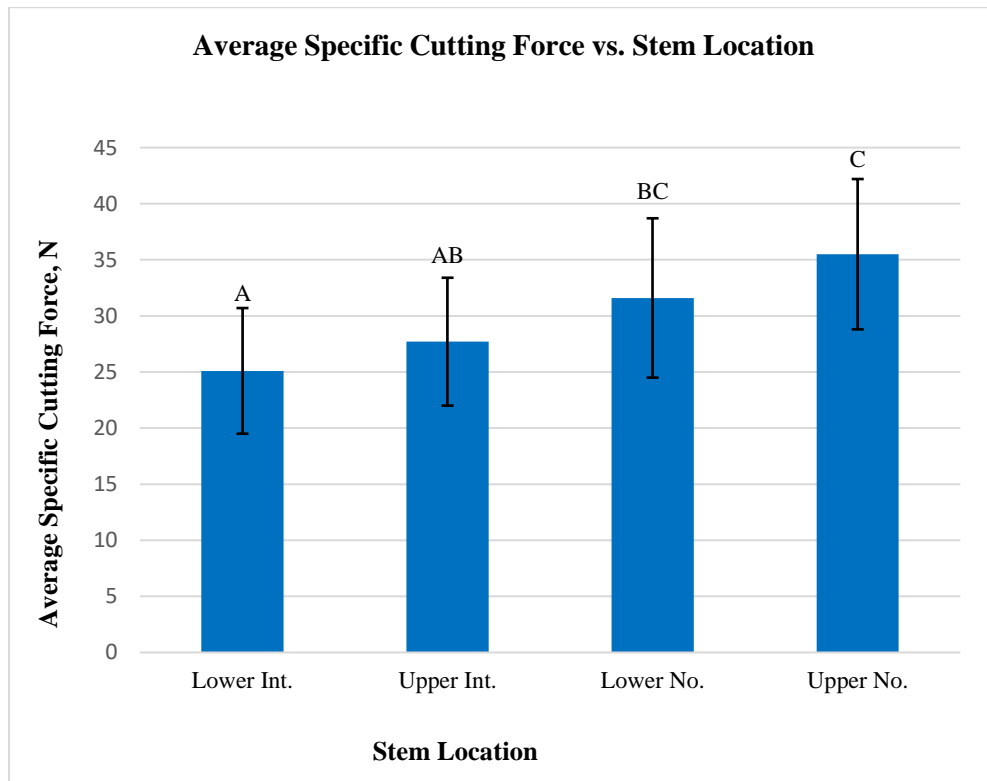


**Figure 5.8 – Effect of stem location on specific cutting force for the flat blade with both sides supported method**

The data of cutting energy and specific energy for a flat blade with both sides supported method are summarized in Table 5.4. The average cutting energy required to cut a single stem is 6.28 J. The lowest average specific cutting energy acquired at the upper node 679.9 J/m, and the highest of 862.8 J/m was at the upper node.

**Table 5.4 – Cutting energy summary for the flat blade with both sides supported method**

Stem Location	Sample Size	Ave. Stem Diameter, mm	Ave. Cutting Speed, m/s	Cutting Energy, J		Specific Cutting Energy, J/m	
				Mean	SD	Mean	SD
Lower Int.	25	8.4	10.7	7.1	3.0	862.8	392
Lower No.	25	9.66	10.9	6.7	2.7	687.5	249.6
Upper Int.	25	7.5	10.8	5.3	1.9	704.8	243.3
Upper No.	25	8.7	10.8	6.0	2.1	679.9	182.7

One-way ANOVA test results for specific energy within 4 stem locations are shown in Figure 5.9. Based on statistical analysis, given that p-value (0.07) is greater than the significance level ( $\alpha=0.05$ ), resulting to fail to reject the null hypothesis. Means of specific cutting energy among the miscanthus stem using a flat blade with both sides supported method are not significantly different.

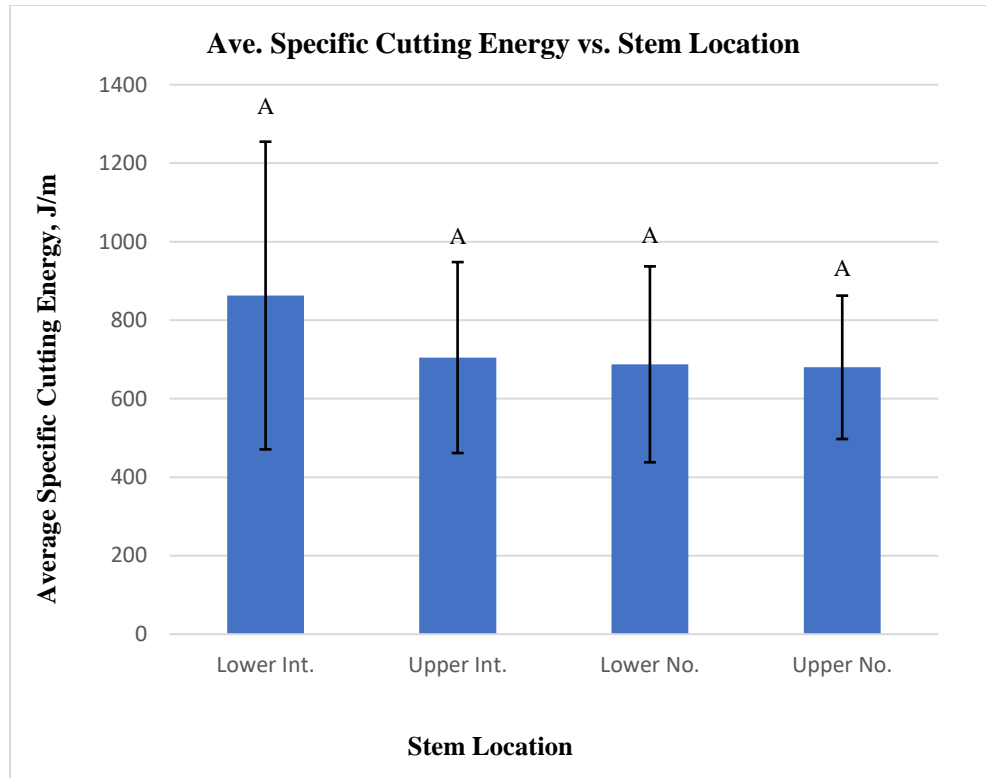


**Figure 5.9 – Effect of stem location on specific cutting energy for the flat blade with both sides supported method**

### **5.3 Serrated blade – one side supported**

The third experiment was conducted using a serrated blade with one side supported cutting method. All samples were randomly selected from two different bundles. The average moisture content of samples was 12.5% (w.b.). The average diameter of the used samples was 9.3 mm, and the average cutting speed was 10.8 m/s. The cut samples using this treatment are shown in Figure 5.10.



**Figure 5.10 – Illustration of cut sample using a serrated blade with one side supported method**

The force-time curve patterns in four locations were similar to the experimental treatments where the flat blade with one side and two sides supported methods were used. Thus, the internodal cutting had a wider force-time curve compared to nodal with sharp and shorter impact time. However, compared to previous treatments, acquired force-time curves in this treatment showed fewer outliers. The average impact cutting time was 0.0019 seconds, which is the same as a treatment where a flat blade with one side supported method was used.

The force-time characteristics of impact cutting in 4 stem locations using a serrated blade with one side supported method are illustrated in Figure 5.11.

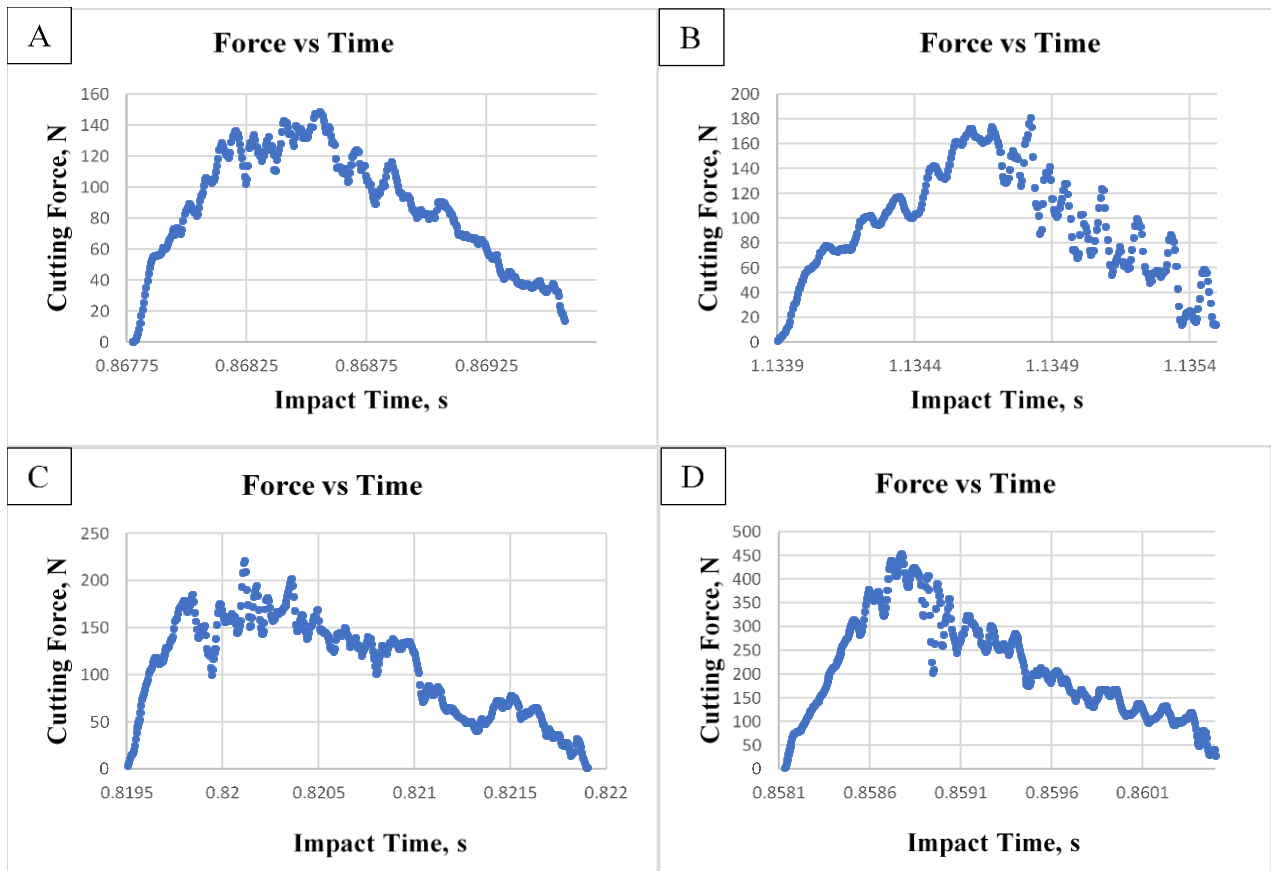


**Figure 5.11 – Force-time curve of cutting in lower int. (A), lower no. (B), upper int. (C), upper no. (D) for the serrated blade with one side supported method**

The specific cutting force slightly decreased when a serrated blade was used. The lowest specific cutting force of 16.8 kN/m was observed at the lower internode, while the highest of 37.8 kN/m at the upper node. The trend in all previous treatments is that the lowest specific force appears at the lower internode and the highest specific force appears at the upper node was continued for this treatment as well. Collected data is summarized in Table 5.5

**Table 5.5 – Peak cutting force summary for the serrated blade with one side supported method**

Stem Location	Sample Size	Ave. Stem Diameter, mm	Ave. Cutting Speed, m/s	Peak Cutting Force, N		Specific Cutting Force, kN/m	
				Mean	SD	Mean	SD
Lower Int.	25	9.1	10.8	156.4	58	16.8	5
Lower No.	25	10.4	10.8	298.7	99	28.2	7.1
Upper Int.	23	8.2	10.7	201.9	82.8	24.5	10.3
Upper No.	24	9.5	10.7	362	157.7	37.8	15.4

Statistical analysis on specific cutting forces showed that means of specific cutting force at least in one location is significantly different from others. In this case, means of specific cutting force in lower and upper internodes are significantly different. Also, means of specific cutting force in lower and upper node sections are significantly different. However, the means of specific cutting force at the upper internode and lower node are not significantly different.

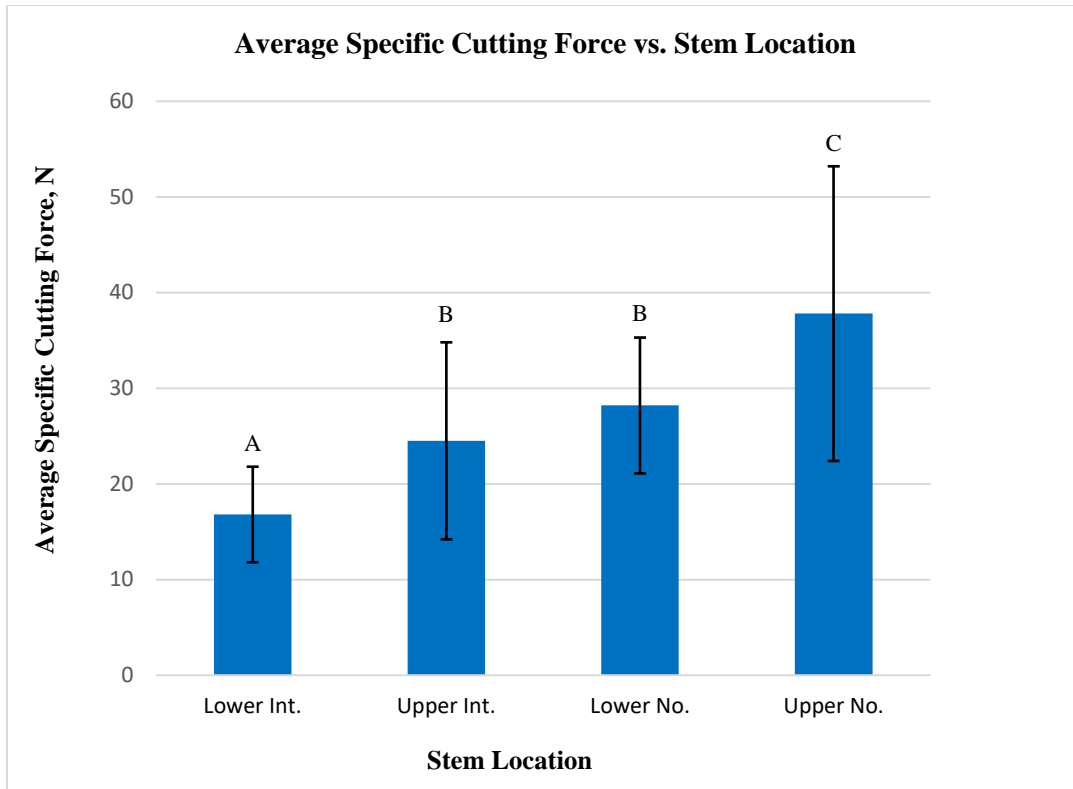


**Figure 5.12 – Effect of stem location on specific cutting force for the serrated blade with one side supported method**

Cutting energy and specific energy data for the serrated blade with one side supported method are summarized in Table 5.6. The average cutting energy required to cut a single stem is 2.98 J. The lowest average specific cutting energy acquired in lower internode of 424 J/m, and the highest of 785.5 J/m was at the upper node.

**Table 5.6 – Cutting energy summary for the serrated blade with one side supported method**

Stem Location	Sample Size	Ave. Stem Diameter, mm	Ave. Cutting Speed, m/s	Cutting Energy, J		Specific Cutting Energy J/m	
				Mean	SD	Mean	SD
Lower Int.	25	9.1	10.8	4	2.9	424	293.7
Lower No.	25	10.4	10.8	6	3.1	551.9	229.8
Upper Int.	23	8.2	10.7	4	2.3	477	261.8
Upper No.	24	9.5	10.7	7.6	3.6	785.5	319.9

One-way ANOVA test results for specific energy within 4 stem locations are shown in Figure 5.13. Based on the statistical analysis, the null hypothesis is failed to be rejected. The mean of cutting energy at least in one stem location is significantly different from others. Means which share the same upper-case letters in Figure 5.13 are not significantly different.

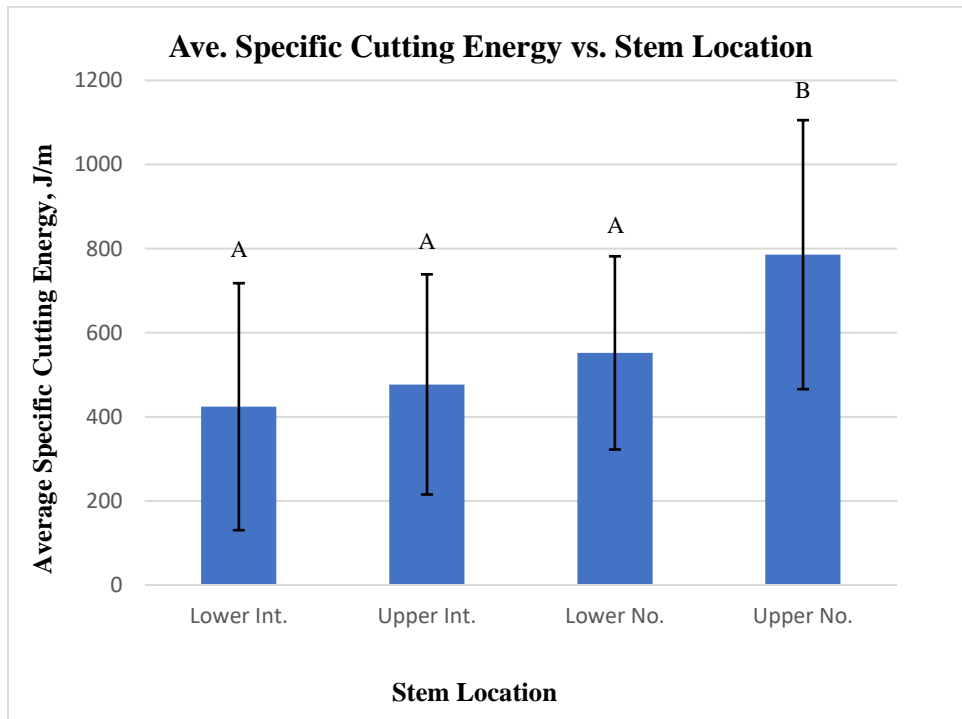


**Figure 5.13 – Effect of stem location on specific cutting energy for the serrated blade with one side supported method**

#### 5.4 Serrated blade – both sides supported

The last experiment was carried out using a serrated blade with both sides supported cutting method. All samples for this treatment were randomly selected from the two different bundles. The average moisture content of samples was 11.4% (w.b.). The average diameter of the used miscanthus specimens was 9.3 mm, and the average cutting speed was 10.9 m/s. During the treatment, effective and clear cutting was obtained as shown in Figure 5.14.



**Figure 5.14 – Illustration of cut sample using a serrated blade with both sides supported method. A- internode section, B – node section**

The force-time curve patterns in four locations were similar to all previous experimental treatments where internodal cutting had a wider force-time curve compared to nodal with sharp and shorter impact time. The average impact cutting time was 0.0021 seconds, which was the highest among the other treatments.

The force-time characteristics of impact cutting in 4 stem locations using a serrated blade with both sides supported method are illustrated in Figure 5.15.

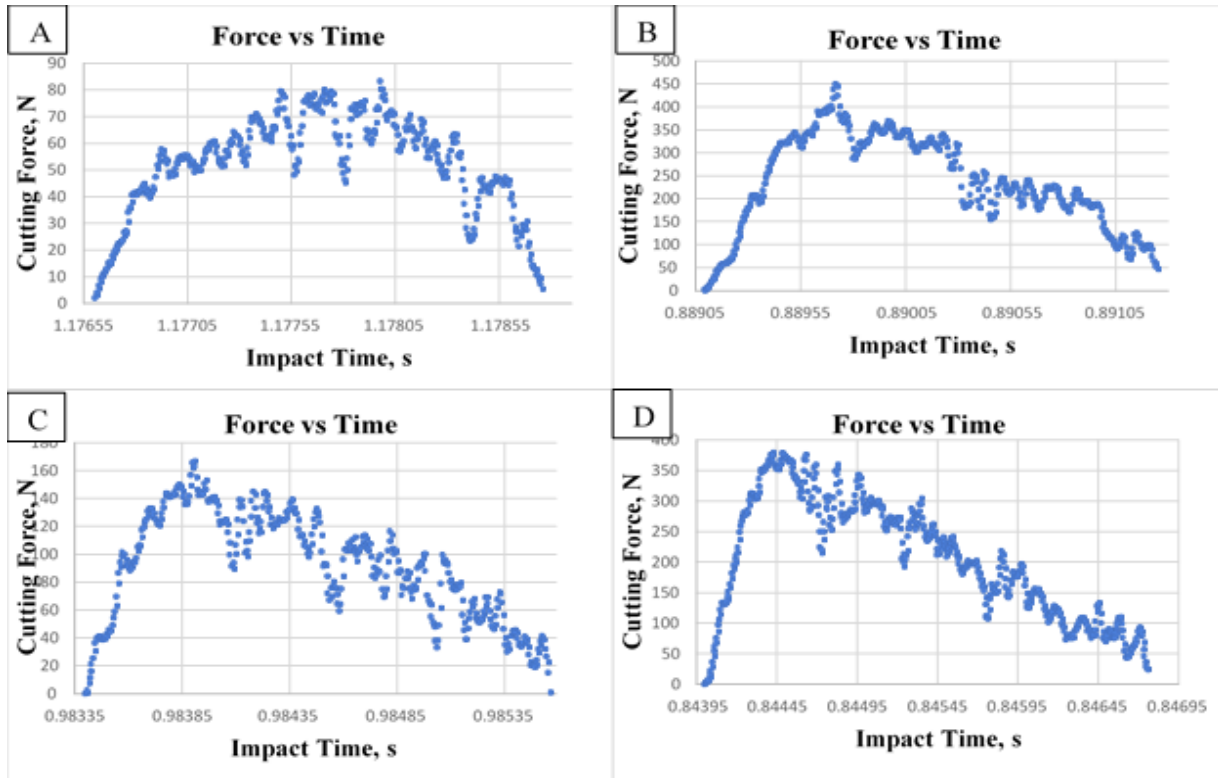


**Figure 5.15 – Force-time curve of cutting in lower int. (A), lower no. (B), upper int. (C), upper no. (D) for the serrated blade with both sides supported method.**

Collected data of peak cutting force, cutting speed, and sample diameter using a serrated blade with both sides supported method are summarized in Table 5.7.

For the serrated blade with both sides supported method, specific cutting force slightly decreased to 5% compared to one side supported method. The lowest specific cutting force of 17.9 kN/m was observed at the lower internode section, while the highest of 32.3 kN/m at the upper node section.

**Table 5.7 – Peak cutting force summary for the serrated blade with both sides supported method**

Stem Location	Sample Size	Ave. Stem Diameter, mm	Ave. Cutting Speed, m/s	Peak Cutting Force, N		Specific Cutting Force, kN/m	
				Mean	SD	Mean	SD
Lower Int.	24	9.1	10.9	165.8	58.2	17.9	4.3
Lower No.	24	10.5	10.8	310.5	101.7	28.9	6.2
Upper Int.	24	8.3	10.8	186.5	48.7	22.4	3.7
Upper No.	24	9.4	10.9	308.8	95.3	32.3	6.8

One-way ANOVA test results for specific force within 4 stem locations are shown in Figure 5.16. The statistical analysis resulted to fail to reject the null hypothesis. The mean of the cutting force at least in one stem location is significantly different from others. Means which share the same upper-case letters in Figure 5.16 are not significantly different.

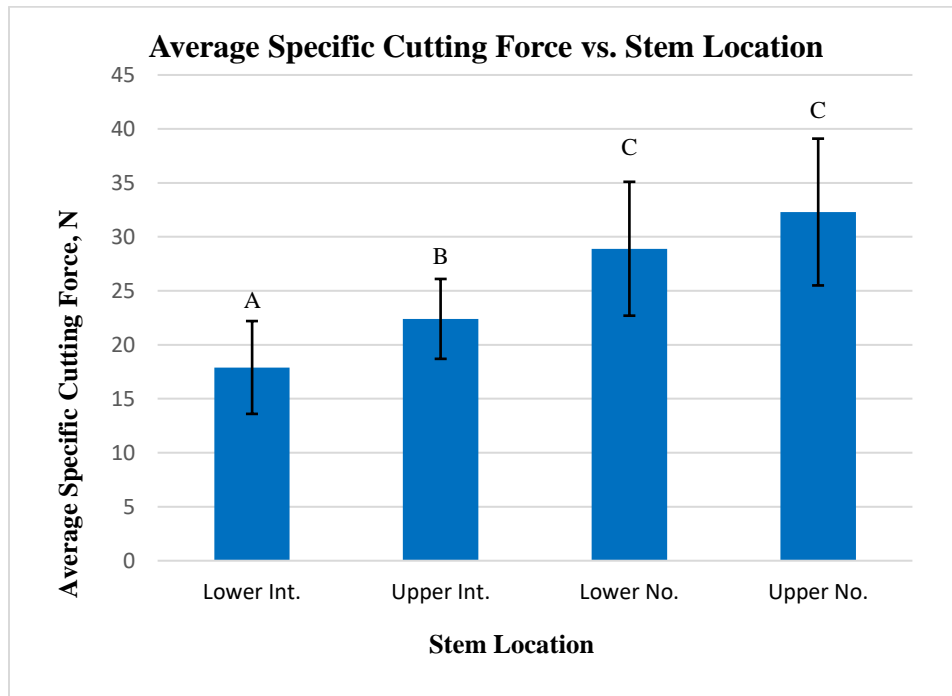


**Figure 5.16 – Effect of stem location on specific peak cutting force for the serrated blade with both sides supported method**

The cutting energy data for the serrated blade with both sides supported method are summarized in Table 5.8. The average cutting energy required to cut a single stem was 2.98 J. The lowest average specific cutting energy acquired in lower internode of 424 J/m, and the highest of 785.5 J/m at the upper node.

**Table 5.8 – Cutting energy summary for serrated blade with both sides supported method**

Stem Location	Sample Size	Ave. Stem Diameter, mm	Ave. Cutting Speed, m/s	Cutting Energy, J		Specific Cutting Energy, J/m	
				Mean	SD	Mean	SD
Lower Int.	24	9.1	10.9	4.6	2	490.2	152.3
Lower No.	24	10.5	10.8	7.4	3.3	680.1	223.6
Upper Int.	24	8.3	10.8	4.7	1.6	559.1	134.3
Upper No.	24	9.4	10.9	7.6	3.1	777.5	230.3

One-way ANOVA test results for specific energy within 4 stem locations are shown in Figure 5.17. Based on statistical analysis, given that p-value is less than the significance level ( $\alpha=0.05$ ), the null hypothesis is rejected. Means of specific cutting energy among miscanthus stem are significantly different at least in one location when the serrated blade with both sides supported method was used.

Means which do not share the same upper-case letters in Figure 5.17 are significantly different. For example, cutting energy means at the lower and upper nodes, and upper internode are not significantly different since they share the same letter based on the statistical analysis.

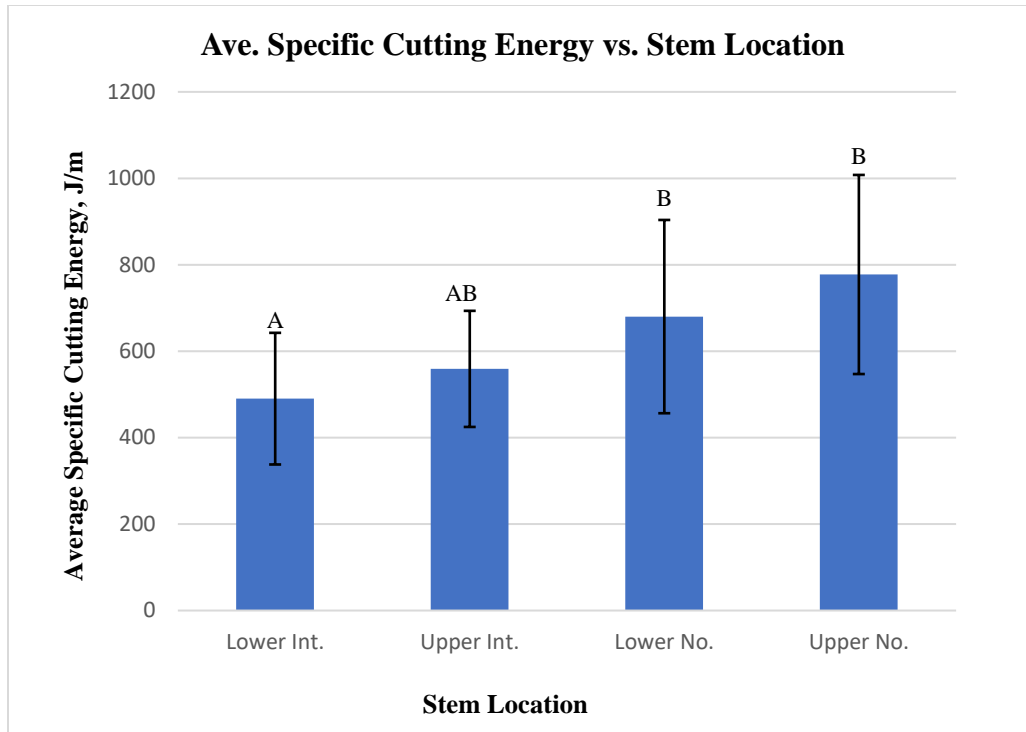


**Figure 5.17 – Effect of stem location on specific cutting energy for the serrated blade with both sides supported method**

### 5.5 Effect of Miscanthus Diameter on Cutting Force

A positive relationship of miscanthus stem diameter was found on cutting force and energy. Cutting force or energy increased with the stem diameter. A strong positive relationship was found between the cutting force and the diameter using the flat ( $R^2=0.42$ ) and serrated ( $R^2=0.42$ ) blades. Moreover, a strong relationship was found between the diameter and cutting energy ( $R^2=0.53$ ) for the serrated blade. However, a weak positive relationship was found between the diameter and cutting energy using a flat blade.

Figure 5.18 illustrates the relationships between the cutting force and miscanthus stem diameter for flat and serrated blades.

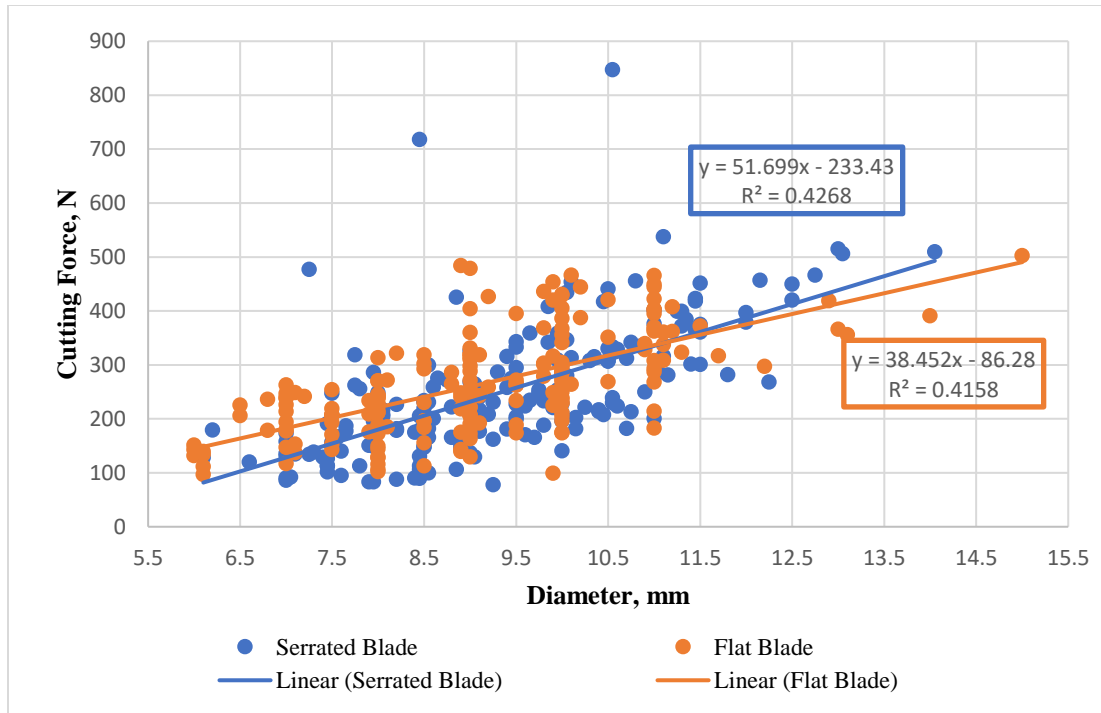


**Figure 5.18 – Effects of miscanthus diameter on cutting force**

## 5.6 Hypothesis testing

In previous sections, each treatment data was individually analyzed in terms of stem location effect on specific cutting force and energy. Based on ANOVA test results, hypothesis testing was conducted. In this section, all collected data were analyzed in terms of blade type and sample supporting method on specific cutting force and energy.

Two sample t-test allows to establish whether or not a flat blade and serrated a blade have an effect on specific cutting force and energy. The null hypothesis states that the means of specific cutting force or energy are equal for the flat blade and the serrated blade. Statistical analysis results of p-value in Table 5.9 less than the significance level of 0.05 concludes to reject null hypothesis.

Results of specific cutting forces and energies at the lower and upper internode sections were significantly different when the both sides supported method was used. Specific cutting force at the lower and upper internode increased by 29% for the flat blade. Moreover, specific cutting energy at the lower internode increased by 43%, and at the upper internode section increased by 21%.

Furthermore, means of specific cutting force at the lower internode are significantly different when one side sample supporting method was used. The specific cutting force increased by 22% for the flat blade.

**Table 5.9 – Statistical analysis results for flat and serrated blades.**

Test #	Blade Type	Supporting Method	Stem Location	P-value	
				Spec. Cutting Force	Spec. Cutting Energy
1	Flat blade	One side supported	Lower internode	0.0093	0.55
	Serrated blade				
2	Flat blade	One side supported	Lower node	0.605	0.525
	Serrated blade				
3	Flat blade	One side supported	Upper internode	0.826	0.358
	Serrated blade				
4	Flat blade	One side supported	Upper node	0.227	0.041
	Serrated blade				
5	Flat blade	Both sides supported	Lower internode	<0.001	<0.001
	Serrated blade				
6	Flat blade	Both sides supported	Lower node	0.165	0.913
	Serrated blade				
7	Flat blade	Both sides supported	Upper internode	0.001	0.0126
	Serrated blade				
8	Flat blade	Both sides supported	Upper node	0.092	0.1
	Serrated blade				

Statistical analysis using 2 sample t-test individually for each treatment was conducted on the sample supporting method. This analysis determined that the sample supporting method had an effect on specific cutting force and energy at 95% confidence interval. The null hypothesis for this analysis states that the means of specific cutting force or energy are equal for the one side, and both sides sample supporting methods. The statistical analysis results for sample supporting methods are shown in Table 5.10. A p-value less than the significance level of 0.05 is considered significant allowing to reject the null hypothesis.

Based on statistical analysis results, the means of specific cutting energy for the flat blade at the lower internode were significantly different, as well as the means of specific cutting force for the flat blade at the upper internode.

Overall, statistical analysis results show that in most treatments the means of specific cutting force or energy for both supporting methods are not significantly different.

**Table 5.10 – Statistical analysis results for one side and both sides sample supporting methods**

Test #	Supporting Method	Blade Type	Stem Location	P-value	
				Spec. Cutting Force	Spec. Cutting Energy
1	One side supported	Flat Blade	Lower internode	0.067	<0.001
			Lower node	0.257	0.1
	Both sides supported		Upper internode	0.138	0.0037
			Upper node	0.338	0.343
2	One side supported	Serrated Blade	Lower internode	0.434	0.329
			Lower node	0.735	0.054
	Both sides supported		Upper internode	0.428	0.173
			Upper node	0.105	0.919

## 5.7 Statistical Analysis

Multiple linear regression analysis allows to measure the effects of independent variables on the response variable. STATA software was used to analyze the effect of independent variables such as blade type, sample supporting method, stem location, and cutting speed on the specific cutting force and energy. The p-value results for independent variables are listed in Table – 5.11. A p-value less than the significance level of 0.05 means that a particular variable is significant in predicting cutting force or energy.

**Table 5.11 – Multiple linear regression analysis results**

Variable	P-value	
	Spec. Cutting Force	Spec. Cutting Energy
Blade type (flat and serrated)	0.01	0.84
Support method (one and both sides)	0.659	0.44
Stem location (internode and node)	<0.001	0.44
Stem location (lower and upper)	<0.001	<0.001
Cutting speed	0.375	0.72
<b>R square</b>	0.30	0.18

Based on regression analysis results, for the specific cutting force blade type, stem locations were statistically significant. However, the sample supporting method and cutting speed were not statistically significant in predicting specific cutting force. In terms of specific cutting energy, only the stem location (internode and node) variable is statistically significant in predicting the response variable.

## 5.8 Discussion

In this section, the results of cutting force and energy using a flat blade and a serrated blade were compared with the previous research results.

The average cutting energy required to cut a single stem of miscanthus, combined for the flat and serrated blades was  $5.8 \pm 2.8$  J. The result agrees with the previous study findings, where the average cutting energy for a flat,  $30^\circ$  and  $60^\circ$  blades was  $9.3 \pm 2.6$  J (Johnson et al., 2012). When comparing the static cutting, the dynamic cutting required more energy to cut a single stem of miscanthus. For example, the average static cutting energy for a flat and serrated flat blade was  $4.1 \pm 0.75$  J (Liu et al., 2012). However, the static cutting required more force than dynamic cutting. For instance, the average specific static force collected by Liu et al. (2012) was 68.5 kN/m, while the average specific dynamic cutting force collected in this research was 27.4 kN/m.

The average specific cutting energy at the node section using a flat blade was  $647.6 \pm 191.3$  J/m. Compared to previous experiment results, the specific cutting energy in node section using a serrated flat blade was  $1057.3 \pm 244.3$  J/m (Johnson et al., 2012). The average specific cutting energy at the internode section using a flat blade was  $644.4 \pm 296.3$  J/m. The specific cutting energy was 44% less than Johnson et al. (2012) results, where the average specific cutting energy at the internode section using a flat blade was  $1151.3 \pm 240.6$  J/m.

Johnson et al. (2012) have conducted a cutting test using a  $30^\circ$  serrated blade only at the internode section. The average specific cutting energy was  $1037.9 \pm 191.7$  J/m. This result was 53% higher than the average specific cutting energy which was collected in this experiment. The average specific cutting energy at the internode section using a  $30^\circ$  serrated blade was  $487.8 \pm 223$  J/m.

## 6 Conclusions and Recommendations

### 6.1 Conclusions

The research was focused on studying interactions between a cutting blade and dedicated energy crop – miscanthus. Since miscanthus is the new potential biomass to the US bioenergy industry, more research needs to be done in order to produce miscanthus on a large scale. Harvesting and size reduction processes have a greater share on cost production. Thus, understanding interactions between a cutting blade and miscanthus stem allows to evaluate harvesting and size reduction processes on a small scale.

In this research, the effects of a blade type, sample supporting method, cutting speed, sample location, and sample diameter on cutting force and energy were studied. The load cell between the hammer and a cutting blade was used to measure the cutting force. Based on force results, cutting energy was calculated using 4.1 and 4.2 formulas. The cutting speed was recorded using the time of flight sensor.

The cutting speed for all treatments ranged between 8 m/s to 11.3 m/s, and the average cutting speed was 10.8 m/s.

The first treatment was carried out using a flat blade with one side sample supporting method. The average diameter of miscanthus samples was 9.65 mm. Overall, the average cutting force required to cut a single stem of miscanthus at the node and internode sections was  $267 \pm 77.8$  N. The cutting energy which was calculated based on cutting force, speed and impact time showed the following results. The combined average cutting energy at the node and internode sections was  $5.4 \pm 1.83$  J.

In the second treatment the flat blade with both sides sample supporting method was used. The average sample diameter of the node and internode section was 8.6mm. The average cutting force recorded at the node and internode sections was  $259 \pm 70.2$  N. The average cutting energy combined at the node and internode sections was  $6.3 \pm 2.4$  J.

In the third experimental treatment a serrated blade with one side sample supporting method was utilized. The average miscanthus stem diameter was 9.3 mm. The average recorded cutting force at the node and internode sections combined was  $254.8 \pm 99.4$  N. The average cutting energy was  $5.4 \pm 2.98$  J.

The last experimental treatment was carried out using a serrated blade with both sides sample supporting method. The average sample used in this treatment was 9.3 mm. The average cutting force at the node and internode sections was  $242.9 \pm 76$  N. The average cutting energy was  $6.1 \pm 2.5$  J.

The cutting force was directly proportional to the sample diameter. Thus, cutting force increased with the stem diameter for the both flat and serrated blades.

Based on the statistical analysis results, the blade type was significant in predicting specific cutting force. The sample supporting method was not significant in predicting cutting force or energy. Stem location, whether it is internode or node, was significant in predicting specific cutting force. The sample location, being whether lower or upper section of the sample, was significant in predicting both specific cutting force and energy. The cutting speed was not significant in predicting specific force and energy, which might be due to the small range of cutting speed, between 8 m/s to 11.3 m/s.

## 6.2 Recommendations

Previous dynamic cutting study on miscanthus (Johnson et al., 2012) was to measure cutting energy at higher cutting speed, which was focused on the calculation of the cutting energy based on kinetic energy loss. The cutting speed ranged from 10 m/s to 20 m/s.

In this research, the recommendation of measuring cutting force was considered. However, due to the limitations and safety concerns of the high-speed impact hammer, exceeding the maximum cutting speed of 11 m/s was not feasible.

As mentioned in previous studies, it is important to find a critical cutting speed which results in minimizing the cutting force and energy. Thus, the next cutting studies on miscanthus should consider cutting speed above 20 m/s. In order to get accurate cutting speed data, it is suggested to use different speed sensors than the time of flight sensor, used in this study.

Two types of cutting blades: 0° flat and 30° serrated blades were used in this experimental study. Since results showed slight difference in cutting force and energy between two blades. The next experimental studies should consider different angled blades, which might result in reduction of cutting force or energy of a single stem miscanthus. For example, in a previous research 60° serrated blade performed better than flat and 30° serrated blades (Johnson et al., 2012).

Moreover, if a cutting device has the vertically rotating arm, similar to the one used in this research, the next experiments should consider that cutting force applied perpendicularly to a sample. Perpendicularly applied force would facilitate on getting accurate cutting results.

## References

- Anderson, E., R. Arundale, M. Maughan, A. Oladeinde, A. Wycislo, and T. Voigt 2011. Growth and agronomy of *Miscanthus X giganteus* for biomass production. *Biofuels* 2(2): 167-183.
- EIA 2013. International energy outlook. Washington, DC: U.S. Energy Information Administration; 2013.
- EIA 2018. "The United States Uses a Mix of Prices - Your Guide to Administration, 16 May 2018, [www.eia.gov/energyexplained/?page=us\\_energy\\_home](http://www.eia.gov/energyexplained/?page=us_energy_home).
- FAO. FAO Stat—forestry database. Geneva, Switzerland: Food and Agriculture Organization of the United Nations; 2013.
- Fasick, G. T., and J. Liu 2015. "A *Miscanthus* Conditioning and Bale Compression Analysis." The Pennsylvania State University.
- Fasick, G. T. 2013. "Effects of Conditioning Methods on Square Bale Density for *Miscanthus* Harversting in Pennsylvania." MS. Thesis, The Pennsylvania State University, University Park, PA.
- Gan, H., S. Mathanker, M. A. Momin, B. Kuhns, N. Stoffel, A. Hansen, and T. Grift 2018. Effects of three cutting blade designs on energy consumption during mowing-conditioning of *Miscanthus Giganteus*. *Biomass and Bioenergy*, 109, 166-171.
- Giampietro, M., S. Ulgiati, and D. Pimentel. 1997. "Feasibility of Large-Scale Biofuel Production. Does an Enlargement of Scale Change the Picture?" *BioScience* 47 (9): 587–600. <http://www.jstor.org/stable/1313165?origin=JSTOR-pdf>.

- Guo, M., W. Song, and J. Buhain. 2015. "Bioenergy and Biofuels: History, Status, and Perspective." *Renewable and Sustainable Energy Reviews* 42: 712–25.  
<https://doi.org/10.1016/j.rser.2014.10.013>.
- Heaton, E. A., F. G. Dohleman, and S. P. Long 2008. "Meeting US Biofuel Goals with Less Land: The Potential of Miscanthus." *Global Change Biology* 14 (9): 2000–2014.  
<https://doi.org/10.1111/j.1365-2486.2008.01662.x>.
- IEA. Resources to reserves 2013. Paris, France: International Energy Agency; 2013.
- IER. Europe's renewable fuel of choice: wood. Washington, DC: Institute for Energy Research; 2013. (<http://www.instituteforenergyresearch.org/2013/04/24/europes-renewable-fuel-of-choice-wood/>).
- Jacobson, M. 2013 "NEWBio Energy Crop Profile: Shrub Willow." Penn State Extension, 22 Aug. 2013, [extension.psu.edu/newbio-energy-crop-profile-shrub-willow](http://extension.psu.edu/newbio-energy-crop-profile-shrub-willow).
- Johnson, P. C. 2012. "Energy Requirements and Productivity of Machinery Used to Harvest Herbaceous Energy Crops." MS. Thesis, University of Illinois at Urbana-Champaign.
- Johnson, P. C., C. L. Clementson, S. K. Mathanker, T. E. Grift, and A. C. Hansen 2012. Cutting energy characteristics of *Miscanthus x giganteus* stems with varying oblique angle and cutting speed. *Biosystems engineering*, 112(1), 42-48.
- Keoleian, G. A., and T. A. Volk 2005. "Renewable Energy from Willow BiomassCrops: Life Cycle Energy, Environmental and Economic Performance." *Critical Review in Plant Sciences* 24 (5–6): 385–406. <https://doi.org/10.1080/07352680500316334>.
- Kofman, P. 2012. Harvesting short rotation coppice willow. *COFORD Harvesting/Transport*, 29, 1-6.

- Kroes, S., and H. D. Harris 1996. "Cutting forces and energy during an impact cut of sugarcane stalks." In CIGR Agricultural Engineering Conference, Madrid, 96A-035. 1996.
- Lin, T., S. Mathanker, L. F. Rodriguez, Y. N. Shastri, A. C. Hansen, and K. C. Ting 2013. Impact of Harvesting Technologies on Biomass Feedstock Logistics. In 2013 Kansas City, Missouri, July 21-July 24, 2013 (p. 1). American Society of Agricultural and Biological Engineers.
- Liu, Q., S. K. Mathanker, Q. Zhang, and A. C. Hansen, 2012. Biomechanical Properties of Miscanthus Stem. Transactions of the ASABE, 55(4), 1125-1131.
- Marrison, D. 2016. "Agronomic Crops Network." Spraying Insecticides on Soybeans and Honey Bees. Agronomic Crops Network, Apr. 2016, [agcrops.osu.edu/newsletter/corn-newsletter/process-harvesting-Miscanthus-northeast-ohio](http://agcrops.osu.edu/newsletter/corn-newsletter/process-harvesting-Miscanthus-northeast-ohio).
- Maughan, J. D., S. K. Mathanker, B. M. Fehrenbacher, and A. C. Hansen 2014. Impact of cutting speed and blade configuration on energy requirement for Miscanthus harvesting. Applied Engineering in Agriculture, 30(2), 137-142.
- O'dogherty, M. J., and G. E. Gale 1991. "Laboratory studies of the effect of blade parameters and stem configuration on the dynamics of cutting grass." Journal of Agricultural Engineering Research 49 (1991): 99-111.
- ORNL. Bioenergy conversion factors. Oak Ridge, TN: Oak Ridge National Laboratory; 2013. [http://bioenergy.ornl.gov/papers/misc/energy\\_conv.html](http://bioenergy.ornl.gov/papers/misc/energy_conv.html)
- Persson, S. 1987. Mechanics of cutting Plant Materials 62, 102,105. St. Joseph, Mich. ASAE.
- Prasad, J., and C. P. Gupta 1975. "Mechanical properties of maize stalk as related to harvesting." Journal of Agricultural Engineering Research 20, no. 1 (1975): 79-87.

Pyter, R., T. Voigt, E. Heaton, F. Dohleman, and S. Long 2007. Growing giant Miscanthus in Illinois. Univ. of Illinois, Urbana-Champaign, IL. Growing giant Miscanthus in Illinois. Univ. of Illinois, Urbana-Champaign, IL.

Shinners, K. J., G. C. Boettcher, R. E. Muck, P. J. Weimer, and M. D. Casler 2010. “Harvesting and Storage of Two Perennial Grasses as Biomass Feedstock” 53 (2): 359–70.

Srivastava, A. K., C. E. Goering, R. P. Rohrbach, and D. R. Buckmaster 2006. Hay and forage harvesting. In Engineering Principles of Agricultural Machines, Second Edition (p. 325). American Society of Agricultural and Biological Engineers.

Technologies, Coal 2013. Resources to Reserves 2013: Oil, Gas and Coal Technologies for the Energy Markets of the Future. Resources to Reserves 2013: Oil, Gas and Coal Technologies for the Energy Markets of the Future. Vol. 9789264090. <https://doi.org/10.1787/9789264090705-en>.

United States Environmental Protection Agency (USEPA), 2016. Inventory of U.S. Greenhouse Gas Emissions and Sinks.

USDA. US bioenergy statistics. Washington, DC: United States Department of Agriculture Economic Research Service; 2013.

USDA ERS - Food Environment Atlas. “Background.” 15 May 2015, [www.ers.usda.gov/topics/crops/corn-and-other-feedgrains/background/](http://www.ers.usda.gov/topics/crops/corn-and-other-feedgrains/background/).

“U.S. Energy Information Administration - EIA - Independent Statistics and Analysis.” Factors Affecting Gasoline Prices - Energy Explained, Your Guide To Understanding Energy - Energy Information Administration, 2 July 2018, [www.eia.gov/todayinenergy/detail.php?id=36612](http://www.eia.gov/todayinenergy/detail.php?id=36612).

- Vu, V.D., Q. H. Ngo, T. T. Nguyen, H. C. Nguyen, Q. T. Nguyen. and V. D. Nguyen 2020.  
Multi-objective optimisation of cutting force and cutting power in chopping agricultural residues. *Biosystems Engineering*, 191, pp.107-115.
- Witzel, C. P., and R. Finger 2016. "Economic Evaluation of Miscanthus Production - A Review." *Renewable and Sustainable Energy Reviews*.  
<https://doi.org/10.1016/j.rser.2015.08.063>.
- Wright, L. 2007. Historical Perspective on How and Why Switchgrass Was Selected as a "Model" High-Potential Energy Crop. Consultancy Work to Bioenergy Resources and Engineering Systems, ORNL/TM-2007/109. <https://doi.org/ORNL/TM-2007/109>.
- Yu, M., A. R. Womac, C. Igathinathane, P. D. Ayers, and M. J. Buschermohle 2006.  
"Switchgrass ultimate stresses at typical biomass conditions available for processing." *Biomass and Bioenergy* 30, no. 3 (2006): 214-219.